Title
The New Face of Cilia: How the Cell's Antenna Coordinates Midfacial Development

Author
Abrams, Shaun

Publication Date
2017

Peer reviewed|Thesis/dissertation

The New Face of Cilia:
How the Cell's Antenna Coordinates Midfacial Development

by

Shaun R. Abrams

DISSERTATION

Submitted in partial satisfaction of the requirements for the degree of

DOCTOR OF PHILOSOPHY

in

Oral and Craniofacial Sciences

in the

GRADUATE DIVISION

of the

UNIVERSITY OF CALIFORNIA, SAN FRANCISCO

Acknowledgements and Dedication

My journey through this exciting ride called graduate school has allowed me to grow and mature both personally and professionally as a budding young scientist. The experience has instilled in me a sense of tenacity, resilience, curiosity and confidence that will undoubtedly be translated into many aspects of my life moving forward. I am both humbled and eternally grateful to have been afforded the opportunity to learn, work, and play in such a stimulating yet challenging environment where my only limits were my creativity and imagination. I leave this phase of my training extremely proud of this body of work, excited to have gone through the journey with the help and tremendous support of those individuals listed below and excited for the new challenges and experiences that lay on the horizon.

I must first thank my parents for their patience, support and encouragement throughout this experience. They taught me through example at a young age the value of hard work and determination while constantly reinforcing that I could do anything I put my mind to. Ill never forget the tremendous pride I felt watching my mom graduate from dental school or helping my dad type his papers for his MBA while I was in high school. When my initial plans to “try out” research for 1 year after undergrad turned into a 5 year research expedition my parents were always incredibly supportive of me following my passions wherever they would lead me. I seldom get the opportunity to tell them how grateful I am for all of the sacrifices they made for my siblings and me so that I could have this once in a lifetime opportunity. I am so proud to be your son.

Along my journey I have been fortunate to have many mentors guide me along this path. The first of these mentors are Dean Mohsin Patwary and Dr. Margaret Carroll from CUNY MEC. They saw an ambitious and eager pre-dental student with a curiosity for science and discovery and planted the seed that maybe I could be a scientist. Lack of exposure to scientists and PhDs who looked like me meant that this possibility wasn't on my radar growing up. I am so glad that I took your advice and the leap of faith to postpone dental school applications and try my hand at biomedical research. The rest is history!

My first foray into research in the PREP scholars program at Johns Hopkins School of Medicine was an eye opening experience. Bumpy at first, I lacked confidence, guidance and mentorship and floundered my first few months in the program. Dr. Rahul Kohli stepped in and took me under his wing showing me the impact a selfless and invested mentor can have on a mentee. Under his guidance my confidence and scientific independence grew tremendously. I will always cherish that opportunity to work and learn from someone that truly inspired me.

My time at the National Institute of Dental and Craniofacial Research was formative in cementing my desire to pursue this challenging yet fulfilling academic route. It was here that I learned all the possibilities and opportunities available in dental research and where my love for developmental and craniofacial biology would be sparked. During this experience I would meet the kind of mentor one could only wish to find once in their career: Dr. Matthew Hoffman. My time spent in the Hoffman lab will no doubt be one of the most enriching experiences of my career. I would have the rare opportunity to work for a mentor that cared as much about my scientific development as well as my personal growth and well-being. I realize how rare of a

quality this is and I am grateful to have had the opportunity to grow in the Hoffman lab. My labmates in the Hoffman lab were also integral to my growth and scientific maturity. In particular, my Postdoctoral mentor Isabelle Lombaert challenged me to think critically and develop my own hypotheses to drive our project and instilled in me the confidence and independent thinking that would serve me extremely well during my PhD studies.

Moving across the country away from family and friends to embark on this journey was a difficult decision to make. Fortunately, I made a tight knit friend group (The original 7, #TO7) that would serve as my family in this new environment. You all listened to me as I vented frustrations over failed experiments, constantly encouraged me when I doubted myself, and provided an outlet for me to have fun and dance my butt off during this grueling program. You helped me fully embody the "work hard, play hard" motto and I can't thank you enough or express how thankful I am to have you all in my life. TO7 crew: Ricky, Corey, Curtis, Jonathan, Gary, and Tyler.

I have had an incredibly supportive thesis committee to guide me through this process. Ralph Marcucio and Nathan Young have been critical in providing me the craniofacial expertise and experimental guidance throughout my project from the early inception up to this point. There is no way I could have been as productive in this endeavor without all of their expertise and assistance. Jeffrey Bush has been tremendously generous with both his time and resources during my PhD studies. He would always make himself available to chat about my scientific progress and would always provide valuable advice about my professional and career objectives. Thank you so much for all of your support!

My time in the Reiter lab is the major reason why my PhD experience has been such a positive and fulfilling one. Working along side such brilliant and supportive colleagues it was a joy to come to lab everyday. Daniel Kopinke, my rotation mentor, constantly pushed me to think critically about my project and offered helpful advice that would allow me to move my project forward at a fast pace. Elle Roberson, I can't express how much I enjoyed talking science and life with you. I laughed SO much in lab because of our interactions, and this levity provided a nice contrast to the day-to-day grind of scientific research.

When the time came to choose a thesis lab my number one criteria was an environment that would best help me grow and nurture my scientific independence. I couldn't ask for a better thesis advisor than Jeremy Reiter. You have been there for me when I needed extra guidance but also allowed me the room and space to grow into an independent thinker. Never lacking in crazy ideas or challenging experiments, you pushed me to think about me project in new and innovative ways. I have no doubt that my experiences in your lab will stand me in great stead for my academic future.

A quote that has held great meaning to me throughout this process is, "Who would you be and what would you do if you weren't afraid". I will forever cherish my decision to embark on this incredible journey in spite of my fears and uncertainty. I can't wait for the next challenge and to see what my future holds….

This thesis is dedicated to MSA. You will never know how much you inspire me!

Abstract

The New Face of Cilia: How the Cell's Antenna Coordinates Midfacial Development

by

Shaun R. Abrams

Primary cilia are ubiquitous microtubule-based organelles that coordinate multiple signaling pathways critical for craniofacial development including Hedgehog, Wnt, and PDGF. Ciliary dysfunction causes a range of human disorders, collectively referred to as ciliopathies, many of which display craniofacial defects such as cleft lip/palate, micrognathia, midface dysplasia, and craniosynostosis. This dissertation explores how defects in the transition zone complex- a ciliary gatekeeper- results in a narrowing or collapse of the midface utilizing transgenic and knockout mouse models. Developmental analysis uncovered that the first molecular defects occur in the prechordal plate, a central organizing center in the developing midface. These early prechordal plate defects were transmitted to the adjacent developing forebrain resulting in a massive increase in cell death and culminating in collapse of the midface. Surprisingly, we could fully rescue the midface defects in multiple transition zone mutants by decreasing *Ptch1* gene dosage. These results have uncovered the molecular underpinnings underlying craniofacial dysmorphology in a group of poorly characterized ciliopathies and hold powerful clinical implications for future strategies aimed at treatment and prevention of these defects.

Table of Contents

List of Tables

List of Figures

Chapter 1:

Introduction

1.1 Overview

The focus of this thesis is elucidating the mechanism by which the primary cilia transition zone complex coordinates normal midfacial development. The introduction chapter provides relevant background information on craniofacial development including key signaling pathways and the various tissues comprising the craniofacial complex, an introduction to primary cilia and its role in the Hh pathway, the role of the transition zone complex as a ciliary gatekeeper, and then reviews what is known about how disruption of ciliary structural or signaling proteins results in human disorders characterized by the presence of craniofacial defects, collectively referred to as craniofacial ciliopathies. It ends with an overview of the relevant organizing centers that regulate midfacial development.

1.2 Craniofacial development

Normal development of the face is an exquisitely complex process that involves signal crosstalk between multiple tissues (neural crest, neurectoderm, mesoderm, and facial ectoderm) to ensure precise coordination of the growth and fusion of the facial primordia; the precursors of the face. In addition to serving as a sensory hub housing multiple sensory organs, the craniofacial complex houses and provides physical protection for the developing brain. Despite the tremendous variation in craniofacial morphology between vertebrate organisms, many of the early events in facial development and signaling molecules that control these events are highly conserved (Liu, Rooker, & Helms, 2010). Below is a description of the early events in craniofacial development relevant to the original work presented later in this thesis.

Among the earliest events in development of the craniofacial complex are the growth and fusion of multiple paired and unpaired facial prominences (also called facial primordia). These consist of the unpaired frontonasal prominence: forming the forehead, nasal septum and bridge of the nose, the medial nasal prominence: forming the premaxilla, philtrum, incisors, and tip of the nose, the lateral nasal prominence: forming the sides of the nose (alae), the paired maxillary prominences which form the upper jaw including maxillary, palatine, zygomatic bones, lateral portions of the upper lip, and molars, premolar, and canines of the maxillary arch, and the paired mandibular prominences which forms the lower jaw structures including the mandible, meckel's cartilage, the lower lip and chin (Burdi, 2006; Chai & Maxson, 2006; J. A. Helms, 2005; Liu et al., 2010). In order for facial development to occur normally, these prominences must grow and fuse in a coordinated manner otherwise craniofacial defects (such as orofacial clefting) can occur. During upper lip development, the medial nasal prominence must fuse with both the

lateral nasal prominence and the maxillary prominence for seamless development. Similarly, during palatogenesis (development of the palate) the palatal shelves (a derivative of the maxillary prominence) initially grow vertically before elevating and growing horizontally where they ultimately meet and fuse at the midline. A defect that prevents either the vertical growth, elevation or fusion of these palatal shelves results in the formation of cleft palate (Bush & Jiang, 2012). Each of the facial prominences is comprised of multiple tissue types (neural crest, paraxial mesoderm, and facial ectoderm), which will be described below.

Sometimes referred to as the 4th germ layer, the neural crest is a multipotent, migratory cell population critical for craniofacial development. Arising from the dorsal aspect of the neural tube- at the junction between the neurectoderm and non-neural ectoderm- neural crest cells (NCC) undergo epithelial-to-mesenchymal transition whereby they migrate along defined stereotypic streams and give rise to various head structures (Knecht & Bronner-Fraser, 2002). The more rostral neural crest population are termed cranial neural crest and are differentiated from the more caudal trunk neural crest population in its ability to differentiate into cartilage, bone and connective tissue (Santagati & Rijli, 2003). After migrating to their final destination, cranial neural crest cells gives rise to many derivatives including the majority of the face and skull bones, parasympathetic ganglia and ganglia of the cranial nerves, melanocytes (pigment cells), Schwann cells of cranial nerves, and connective tissue including dermis, fat and smooth muscle of the skin (Santagati & Rijli, 2003). The importance of this cell population to craniofacial development is underscored by the finding that defects affecting the induction, specification, migration or signaling of neural crest cells results in large class of human disorders

marked by the presence of severe craniofacial defects collectively referred to as neurocristopathies (Etchevers, Amiel, & Lyonnet, 2006).

At the central core of the pharyngeal arches (a series of paired arches giving rise to head and neck structures) lies paraxial mesoderm tissue that will form the majority of the craniofacial musculature. In addition to its role in forming head musculature, the paraxial mesoderm will give rise to bones of the skull including the parietal and occipital bones (Trainor, Tan, & Tam, 1994). Along the pathway of differentiation of the primitive paraxial mesoderm towards a somitic cell fate the paraxial mesoderm gives rise to 3 distinct cell layers: the dermatome, myotome, and sclerotome. The dermatome ultimately gives rise to the dermis, the myotome to all the striated muscles of the body, and the sclerotome to the vertebrate and intervertebral discs (Couly, Coltey, & Le Douarin, 1992).

The tissue covering all facial prominences is the facial ectoderm (also referred to a surface ectoderm). In addition to its role in forming the epidermis- the outer skin layer forming a protective barrier- this tissue is rich in signaling molecules and ligands belonging to multiple pathways critical for directing craniofacial development, including the Hh, Wnt and BMP pathways (Foppiano, Hu, & Marcucio, 2007; Marcucio, Cordero, Hu, & Helms, 2005; Reid, Yang, Melvin, Taketo, & Williams, 2011). The close apposition of the facial ectoderm to the underlying mesenchyme has uncovered critical signaling crosstalk between these two tissues. In numerous instances, signals produced by the facial ectoderm are received and interpreted by cells of the cranial mesenchyme to regulate cellular processes in the mesenchyme including growth, differentiation, and migration (Marcucio et al., 2005).

1.3 Primary cilia and the Hedgehog pathway

Primary cilia are microtubule-based organelles projecting from the surface of almost every vertebrate cell. Initially thought of as vestigial structures with no important function, over the past decade a mountain of data has uncovered the critical roles primary cilia play in normal development and, when disrupted, in human disease and cancer. Underscoring the importance of primary cilia is the growing list of human disorders affecting diverse organ systems caused by either structural or functional defects in cilia, collectively referred to as ciliopathies. Analysis into the distinct protein composition of the ciliary membrane has revealed that primary cilia are important for the regulation of key developmental pathways including the hedgehog (Hh) pathway.

The hedgehog pathway is a highly conserved pathway critical for the development of many tissues/organs including neural tube patterning, limb development and craniofacial morphogenesis. In addition to its important role during development, the Hh pathway must be carefully regulated in adults as hyperactivation can lead to human cancers including basal cell carcinoma (BCC) and medulloblastoma. The Hh family of proteins contains three members in vertebrates: Sonic hedgehog (Shh), Indian hedgehog (Ihh), and Desert hedgehog (Dhh). Each member in encoded by a *Hh* gene and the *Hh* transcripts are translated into proteins of ~45 kD which are processed ultimately into lipid-modified ligands of ~19 kD. These Hh ligands are secreted and can act on the cell in which they were produced in an autocrine manner, on neighboring cells in a paracrine manner, or on cells far from its source. In the absence of ligand stimulation the pathway is effectively off: Ptch (a twelve-pass transmembrane receptor) inhibits the effector receptor of the pathway Smo (a seven-pass transmembrane GPCR-like receptor)

leading to the processing of the Gli family of transcription factors into a predominantly repressor form to turn of Hh pathway targets. Upon ligand stimulation, the Hh ligand binds to the Ptch receptor, relieving Ptch repression of Smo leading to processing of the Gli transcription factors into the activator form ultimately leading to active transcription of Hh target genes.

Several lines of evidence have uncovered the links between the Hh pathway and primary cilia in vertebrates. The first piece of evidence was the result of a phenotypic screen for mouse mutants displaying defective patterning. Identifying mutants with defects similar to Hh loss-of-function mutants revealed a surprising culprit: mutations in the intraflagellar transport (IFT) machinery (Huangfu & Anderson, 2005; Huangfu et al., 2003). This IFT machinery is critical for the extension and maintenance of the cilium via transport of cargo along the ciliary axoneme (Eggenschwiler & Anderson, 2007; S. Kim & Dynlacht, 2013; Pedersen & Rosenbaum, 2008). A second piece of evidence connecting cilia and the Hh pathway is the discovery that many major components of the pathway are enriched in the cilium. These include the two receptors of the pathway Ptch and Smo, the transcription factors Gli2 and Gli3, and the negative pathway regulator Sufu. The two transmembrane receptors have been found to localize to the cilium in a dynamic fashion. In absence of ligand stimulation, Ptch1 is enriched in the cilium and prevents Smo localization to the cilium (Rohatgi, Milenkovic, & Scott, 2007). Upon ligand stimulation, Ptch1 exits the cilium and Smo enters and becomes enriched in the cilium (Corbit et al., 2005). Also in response to ligand stimulation the predominant transcriptional activator Gli2 and the predominant transcriptional repressor Gli3 are reported to accumulate at tip of the cilium (Endoh-Yamagami et al., 2009; J. Kim, Kato, & Beachy, 2009).

1.4 The transition zone complex: A ciliary gatekeeper

In order for the primary cilium to function as a specialized signaling organelle of the cell there must be mechanisms in place to ensure selective access and maintenance of key ciliary proteins. This selective barrier must be able to discriminate and identify which soluble and membrane proteins should gain access to the cilium and which proteins should be excluded from the cilium. Further complicating this task is the dynamic nature of ciliary signaling whereby the ciliary protein composition exhibits rapid changes during various signaling states within the cilium. As this regulation of ciliary protein composition is disrupted in many ciliopathies, numerous groups have worked over the past decade to uncover the modes of regulation for ciliary access. These studies have uncovered distinct mechanisms for the ciliary access of soluble versus membrane proteins.

Analysis into the cilia of retinal pigment epithelial cells provided evidence for the presence of a size exclusion barrier restricting ciliary access of soluble proteins. Whereas dextrans 10 kD or smaller were able to enter the cilium in these cells, dextrans 40 kD or larger did not gain access to the cilium (Kee et al., 2012). Additional lines of evidence have identified nuclear pore proteins at the base of cilia and showed the requirement of importins for the ciliary entry of specific soluble proteins arguing that parallels exist between the mechanisms of ciliary and nuclear pore entry (Dishinger et al., 2010; Hurd, Fan, & Margolis, 2011; Kee et al., 2012).

The transition zone complex is a complex of ciliopathy proteins that form Y-link structures at the ciliary base between the basal body and ciliary axoneme to regulate ciliogenesis and ciliary membrane protein composition (Garcia-Gonzalo & Reiter, 2012). Interestingly, the transition

zone complex is required for ciliogenesis in a tissue-dependent manner. Whereas cilia were shorter and fewer in the node and neural tube of TZ mutants, ciliogenesis was normal in the notochord, limb mesenchyme and perineural mesenchyme of these same mutants (Garcia-Gonzalo et al., 2011). The complex is made up of two distinct sub-complexes: the MKS-JBTS complex consisting of ciliopathy proteins mutated in Meckel and Joubert Syndromes and the NPHP complex consisting of ciliopathy proteins mutated in Nephronopthisis. The list of genes encoding proteins that comprise the MKS-JBTS sub-complex of the transition zone are *Tctn1, Tctn2, Tctn3, Mks1, Tmem216, Tmem67, Cep290, B9d1, B9d2, Cc2d2a, Tmem231, and Tmem17.* Meckel and Joubert syndromes display classic ciliopathy phenotypes including craniofacial, brain, limb and kidney defects whereas NPHP patients present with cystic kidneys. Genes encoding proteins that comprise the NPHP sub-complex of the transition zone include *Nphp1, Nphp4, Nphp8, Nek8, Nphp3, Invs, Nphp5*, and *Atxn10* (Garcia-Gonzalo & Reiter, 2012). While proteomic analysis uncovered the extensive protein networks of these distinct complexes, genetic perturbation of various transition zone components through the generation of mutant mice and in *C.elegans* mutants uncovered how the transition zone functions in regulating ciliary membrane composition. Loss-of-function mutants for various MKS-JBTS components revealed that when this complex is disrupted ciliary membrane proteins including Arl13b, AC3, Smo, and Pkd2 fail to localize to the primary cilium (Ben Chih et al., 2011; Dowdle et al., 2011; Garcia-Gonzalo et al., 2011; Roberson et al., 2015). In addition to the loss of ciliary localization of these proteins was a failure to restrict non-ciliary membrane proteins from entering the cilium (Ben Chih et al., 2011). Although we now presumably know most of the components and functions of this critical ciliary gatekeeper we are only just beginning to learn how this complex performs this gatekeeper function.

1.5 Craniofacial ciliopathies

Given the ubiquitous nature of primary cilia and its role in the development of a diverse array of cells, tissues and organs it is easy to see how defects in the structure or function of this signaling organelle leads to human syndromes characterized by defects in numerous tissues and organ systems. Some ciliopathy phenotypes such as holoprosencephaly and polydactyly seen in Meckel syndrome and skeletal defects affecting the limbs and ribs seen in Ellis-van-Crevald syndrome have been linked to defects in the Hh pathway (Goetz & Anderson, 2010). Other defects such as retinal degeneration, anosmia (loss of smell) and hearing loss have been attributed to the function of cilia in specialized cell types: the photoreceptor connecting cilia, sensory neurons in the olfactory epithelium and cilia of the cochlea, respectively (Kulaga et al., 2004; Nishimura et al., 2004). As cilia have dual roles in both signaling and motility some of the defects seen in ciliopathy patients such as sterility, hydrocephalus (excess buildup of cerebrospinal fluid in the brain), and chronic lung infections seen in primary ciliary dyskinesia can be attributed to defects in the motile function of cilia (Baker & Beales, 2009). While these ciliopathy phenotypes have been heavily investigated over the past decade another common phenotype seen in ciliopathy patients that is currently poorly understood is the presence of craniofacial defects. The human ciliopathies that display craniofacial defects are termed craniofacial ciliopathies and by some estimates these defects are seen in approximately one-third of all ciliopathy patients. The following is a summary of what is currently known about the craniofacial ciliopathies and the craniofacial anomalies associated with each syndrome.

Meckel syndrome (also called Meckel-Gruber syndrome) is an autosomal recessive disorder on the severe end of the ciliopathy phenotypic spectrum. This perinatal lethal disorder is

characterized by holoprosencephaly or impaired cleavage of the embryonic forebrain, left-right patterning defects such as situs inversus and heterotaxy, congenital heart defects, polycystic kidney disease, polydactyly, and the presence of many craniofacial defects including hypotelorism or narrowing of the facial midline, cleft lip/palate, occipital encephalocoele, microcephaly, micrognathia, sloping forehead, and tongue malformations (Ahdab-Barmada & Claassen, 1990; Boycott et al., 2007; Cakir, Mungan, Makuloglu, & Okten, 2006; Cui et al., 2010; Dowdle et al., 2011; Garcia-Gonzalo et al., 2011). Most of the causative mutations found in this syndrome are attributed to genes that encode proteins localizing to the ciliary transition zone, namely *TCTN1, TCTN2, CC2D2A, MKS1, B9D1, B9D2, TMEM231, TMEM67, CEP290, NPHP8 and NPHP3* (Baala et al., 2007; Delous et al., 2007; Dowdle et al., 2011; Garcia-Gonzalo et al., 2011; Kyttälä et al., 2006; Roberson et al., 2015; Roume et al., 1998; Smith et al., 2006). How defects in the ciliary transition zone leads to the craniofacial defects seen in Meckel syndrome is currently unknown with evidence for the etiology of the midface defects provided in this thesis.

Joubert syndrome is an autosomal recessive disorder characterized by cerebellar vermis hypoplasia, developmental delay, ataxia or loss of control of body movements, polydactyly, retinal degeneration, and renal cysts. Craniofacial abnormalities include cleft lip/palate, hypertelorism, long face and frontonasal prominence, prognathism, and a prominent nasal bridge and tip (Maria, Boltshauser, Palmer, & Tran, 1999). Causative loci have been linked to many genes including *CC2D2A, NPHP1, AHI1, CEP290, RPGRIL1L, TMEM67, ARL13B,* and *TMEM216* (Cantagrel et al., 2008; Edvardson et al., 2010; Garcia-Gonzalo et al., 2011; Maria et al., 1999; Sayer et al., 2006). Phenotypic variability and overlap with other syndromes have

made clinical diagnosis of Joubert patients particularly challenging. To date, mechanistic analysis into the cause of these many craniofacial defects has not been described.

Ellis-van-Creveld syndrome is a chondroectodermal dysplasia characterized by dysplasia of the nails and teeth and anomalies of skeletal and craniofacial tissues. Skeletal features include short limbs and short ribs while craniofacial abnormalities include supernumery labiogingival frenulae and defects in dentition such as premature tooth eruption, missing primary and permanent teeth or edentulism, and the presence of underdeveloped, small conical teeth (Cahuana, Palma, Gonzáles, & Geán, 2004; Susami, Kuroda, Yoshimasu, & Suzuki, 1999). Positional cloning has identified two loci: the genes *EVC* and *EVC2* (Galdzicka et al., 2002; Polymeropoulos et al., 1996; Ruiz-Perez et al., 2000). The Evc proteins have been found to form a complex with the Smo receptor and to be required for robust Hh signal transduction (Dorn, Hughes, & Rohatgi, 2012). In regards to the long bone defects in *Evc* mutants, the protein has been found to function as a positive regulator of Ihh-regulated bone growth (Ruiz-Perez et al., 2007).

As its name suggests, Oro-facial-digital syndrome is characterized by abnormalities affecting the oral cavity, face and digits. This syndrome is marked by high phenotypic heterogeneity and is classified into fourteen subgroups: OFD Type I through OFD type XI. While the inheritance pattern of OFD type 1 is X-linked dominant, most other OFD types display autosomal recessive pattern of inheritance. Craniofacial malformations are present in almost 70% of cases and include cleft lip/palate, hypertelorism, microretrognathia, hypoplasia of the ala nasi, flat face, and low-set ears. Oral abnormalities describes include aberrant frenula, tongue abnormalities, high-arched palate, abnormalities in tooth number and enamel formation, clefts of the alveolar

ridge, and lingual hamartomas. The causative mutation for OFD type 1, *OFD1*, has been found to cause defects in ciliogenesis and neural tube patterning highlighting a ciliary role for dysmorphology. Additionally, two additional OFD genes, *TMEM231* and *TMEM107*, have been found to function as critical components of the ciliary transition zone (Roberson et al., 2015; Shylo, Christopher, Iglesias, Daluiski, & Weatherbee, 2016).

Bardet-Biedl Syndrome (BBS) is an autosomal recessive disorder characterized by mental retardation, obesity, polydactyly, cystic kidneys, and retinal degeneration. BBS exhibits phenotypic heterogeneity and has been linked to 14 loci including *MKS1, CEP290,* and *BBS1-12*. Craniofacial defects include hypertelorism, deep-set eyes, downward slanting palpebral fissures, and a flat nasal bridge. In a zebrafish model, craniofacial defects including micrognathia, cyclopia and shortening of the anterior neurocranium in *Bbs8* morphants were attributed to defects in neural crest migration (Tobin et al., 2008). Mechanistic analysis into the cellular function of the protein products of BBS genes suggests these proteins form a coat complex similar to COP1, COPII and clatharin coats to traffic receptors such as the somatostatin receptor SSTR3 and Neuropeptide Y family receptors to the primary cilium (Jin et al., 2010; Loktev & Jackson, 2013).

Cranioectodermal dysplasia (CED), also known as Sensenbrenner Syndrome, is an autosomal recessive disorder characterized by ectodermal, craniofacial, kidney and skeletal defects. Craniofacial defects associated with this syndrome include sagittal craniosynostosis, hypodontia or microdontia, retrognathia, high-arched palate, multiple oral frenula, hypertelorism, and a flat prominent forehead (Konstantinidou et al., 2009; I. D. Young, 1989). The discovery of two genes

encoding proteins involved with IFT transport (*Ift122* and *Wdr35)* as causative loci has sparked great interest into the mechanism of this relatively new ciliopathy (Konstantinidou et al., 2009; Walczak-Sztulpa et al., 2010).

1.6 Organizing Centers Regulating Midfacial Development

The identification of organizing centers- tissues capable of influencing the fate or function of an adjacent responding tissue- has been one of the most exciting discoveries in the field of developmental biology in the past century. Pioneering work by Spemann and Mangold provided the first concrete evidence for the existence of such organizers when they demonstrated that a graft of dorsal blastopore lip could exert an inductive effect on its host tissue to cause the formation of a secondary embryo (Spemann & Mangold, 2001). Following this discovery, a number of organizing centers have been identified in the embryo including the notochord, floor plate and the zone of polarizing activity (ZPA). The notochord is an axial mesendoderm derivative of the dorsal blastopore that is critical for the induction of ventral cell types in the neural tube including the floor plate and motor neurons (C. Anderson & Stern, 2016; Sulik et al., 1994). Experimental extirpation of the notochord leads to loss of floor plate specification and ventral neural cell types while grafting notochord tissue adjacent to the lateral neural tube transforms this tissue into ventral cell types. This ability of the notochord in the direct induction and patterning of ventral cell types and the capacity to re-direct cells and tissues into this cell fate confirms that this tissue is a bonafide organizer. Similar experiments carried out using grafts of floor plate tissue have confirmed that this tissue also contains organizer capability in its ability to induce ventral cell types in the lateral neural tube. Similarly, two organizing centers have been identified in the developing limb: the zone of polarizing activity (ZPA) and the apical ectodermal ridge (AER). Both organizing centers are dependent on the other for its maintenance and grafting of each organizing center results in mirror-image duplication of structures. The rest of this section describes three organizing centers that are critical for regulating development of the

midface: the prechordal plate, a signaling center in the ventral forebrain, and the frontonasal ectodermal zone (FEZ).

The axial mesendoderm, named for its location in the ventral midline of the embryo and its contribution to both mesoderm and endoderm derivatives, is comprised of the notochord plate at the posterior region and the prechordal plate at the anterior tip. Similar to the function of the notochord in induction of the adjacent neurectoderm into the floor plate and ventral cell types, the prechordal plate exerts its organizing activity on the adjacent neurectoderm to induce forebrain patterning and the development of anterior head structures. Consistent with the common theme of organizers expressing soluble ligands to exert their inductive effect on adjacent tissues, the prechordal plate is rich in these growth factors including Shh and Bmp7. Extirpation studies have revealed the organizer function of the prechordal plate in regulating midfacial development. Surgical removal of the prechordal plate in rat embryos and subsequent whole embryo culture resulted in loss of a critical signaling center in the ventral forebrain evidenced by reduced *Shh* and *Nkx2.1* expression and severe narrowing/collapse of the facial midline (Aoto et al., 2009).

The old adage, "The face predicts the brain" signifies the long-held realization that development of the face and brain are intimately connected. Supporting this assertion, a *Shh*-expressing signaling domain in the ventral telencephalon has been shown to regulate outgrowth of the developing midface and upper jaw (Marcucio et al., 2005). Inhibiting Shh signaling in this tissue resulted in defects in the dorsoventral polarity of the forebrain via loss of ventral markers *Nkx2.1* and *Dlx2* and subsequent narrowing of the midface. Further evidence supporting an organizer

role for this Shh signaling center in the ventral forebrain lies in its ability to induce the expression and formation of an adjacent signaling center in the facial ectoderm marked by expression of Shh and Bmp ligands. Complementing loss-of-function studies for this forebrain organizer are gain-of-function studies via ectopic application of Shh to the ventral forebrain and corresponding expansion of the facial midline (Hu & Marcucio, 2008). Furthermore, midfacial width could be modulated, either expansion or narrowing, via dose-depended activation or inhibition of the Hh pathway in the ventral forebrain (N. M. Young, Chong, Hu, Hallgrimsson, & Marcucio, 2010).

Investigation into the role of the facial ectoderm in regulating midface outgrowth has uncovered a third organizing center in the developing craniofacial complex, the frontonasal ectodermal zone (FEZ). Removal of this tissue or inhibition of Shh signaling in the FEZ results in growth arrest in the underlying mesenchyme and a corresponding reduction in midface outgrowth (D. H. A. J. A. Helms, 1999). In addition to this role in mediating midface outgrowth, the FEZ has been demonstrated to confer dorsoventral patterning in the developing frontonasal prominence (Hu, 2003). Further evidence confirming the inductive potential of this tissue is provided by its ability to re-pattern the mandible in the formation of an ectopic cartilaginous outgrowth (Hu, 2003). In addition to Shh, the FEZ is rich in other growth factors including Bmp4, Bmp7, and Wnts that also play a role in mediating midfacial development.

Although introduced and discussed separately, the three organizing centers with roles in midfacial development described here are highly dependent on one another for their formation, maintenance and function. Formation of each organizing center occurs in a step-wise manner

such that the earliest signaling center (the prechordal plate) induces the formation of the adjacent organizer in the ventral forebrain, that in turn leads to the formation of the FEZ in the overlying ectoderm. This sequential activation of each signaling center must be tightly regulated to ensure normal midfacial development.

Chapter 2:

The primary cilia transition zone complex mediates signal crosstalk from the prechordal plate to the neurectoderm to coordinate midfacial development

2.1 Abstract

The presence of craniofacial defects such as cleft lip/palate, midface defects, jaw disorders, tooth abnormalities and tongue defects are among the most common phenotypes seen in ciliopathy patients, however the underlying molecular etiology is currently poorly understood. Utilizing multiple transition zone mutant mouse models (*Tctn2, Cc2d2a, Tmem231, and Tmem67)* we have uncovered the molecular pathways and corresponding defects that drive the development of hypotelorism; a midface defect characterized by a narrowing/collapse of the facial midline. We traced the earliest causative defect to the head organizer, the prechordal plate, with reduced marker expression and Hh pathway activation in *Tctn2* mutants. This early prechordal plate defect was transmitted to the adjacent neurectoderm leading to loss of a critical *Shh* domain in the ventral forebrain and reduced Hh pathway activation in this tissue. This resulted in a massive increase in cell death in both the neurectoderm and facial ectoderm via a caspase-9/caspase-3 dependent mechanism culminating in a severe narrowing of the midface. Interestingly, decreasing *Ptch1* gene dosage rescued the midface defect in both *Tctn2* and *Cc2d2a* mutants by decreasing cleaved-caspase3/9 induced cell death. These results identify a new role of the transition zone in mediating key signaling crosstalk between the prechordal plate and the neurectoderm in midfacial development and identify *Ptch1* as a new therapeutic target in treating ciliopathy-associated midface defects.

2.2 Introduction

Primary cilia are ubiquitous microtubule-based organelles present on nearly every cell type in vertebrates critical for the development of a diverse array of cells and tissues. Over the past decade the role of primary cilia as specialized cellular signaling organelles has been identified as they coordinate multiple signaling pathways critical for development including Hedgehog, Wnt, and PDGF pathways (Zaghloul & Brugmann, 2011). Defects in the structure or signaling function of cilia have been linked to a group of human syndromes, collectively referred to as ciliopathies, with a wide spectrum of phenotypes including cystic kidneys, retinal degeneration, cognitive impairment, respiratory defects, left-right patterning defects, polydactyly, and skeletal defects (Baker & Beales, 2009; Schwartz, Hildebrandt, Benzing, & Katsanis, 2011; Tobin & Beales, 2009). In addition to these phenotypes the presence of craniofacial defects is a common feature among ciliopathies, seen in approximately one-third of patients. These defects include cleft lip/palate, high-arched palate, jaw disorders, midface dysplasia, craniosynostosis, tongue abnormalities, abnormal dentition and tooth number, and exencephaly (Brugmann, Cordero, & Helms, 2010b; Zaghloul & Brugmann, 2011). The underlying molecular etiology responsible for the majority of these craniofacial abnormalities remains poorly understood.

How primary cilia can give rise to seemingly opposing phenotypes such as midfacial narrowing/collapse (hypotelorism) and midfacial expansion (hypertelorism) has been an active area of both interest and confusion. While a mechanism involving loss of Gli3 repressor function in the neural crest has been described to explain the hypertelorism phenotype, not much is known regarding how ciliary dysfunction leads to midface collapse (Brugmann et al., 2010a; Liu, Chen, Johnson, & Helms, 2014). Additionally, it has been discovered that disruption of the Gli3

activator: Gli3 repressor ratio in the *talpid*^{2} avian mutant leads to increased Gli3 activator levels specifically in the frontonasal prominence resulting in widening of the midface (Chang et al., 2014).

Investigation into the role of the Hh pathway in forebrain and midface development indicates that mutations leading to decreased pathway activation results in impaired midline cleavage of the forebrain and corresponding narrowing of the midface (Fuccillo, Joyner, & Fishell, 2006; D. H. A. J. A. Helms, 1999; Hu & Marcucio, 2008; Marcucio et al., 2005; Muenke & Beachy, 2000; N. M. Young et al., 2010). Mutations in *Shh* lead to holoprosencephaly, the most common congenital forebrain malformation characterized by incomplete cleavage of the embryonic forebrain (Chiang et al., 1996; Cohen & Shiota, 2002). Meckel syndrome (MKS), a severe perinatal lethal ciliopathy, has also been characterized by the presence of holoprosencephaly and midfacial narrowing/collapse (Ben Chih et al., 2011; Dowdle et al., 2011; Garcia-Gonzalo et al., 2011). MKS associated genes encode proteins that form a complex at the base of cilia, termed the transition zone, to regulate ciliogenesis and ciliary membrane protein composition in a tissue-specific manner (Ben Chih et al., 2011; Dowdle et al., 2011; Garcia-Gonzalo et al., 2011; Roberson et al., 2015). While defects in the Hh pathway has been invoked to explain the forebrain and midface defects in transition zone cilia mutants, there is a lack of detailed experimental evidence to support this claim.

In this study we set out to uncover the molecular etiology driving the development of forebrain and corresponding midface defects utilizing multiple transition zone mouse mutants including *Tctn2, Cc2d2a,* and *Tmem231*. We found that the forebrain and midface defects are present early

during development, as early as E9.5, and persisted throughout early development. We were able to trace the tissue and timepoint where defects are first apparent to the prechordal plate, a central organizing center for development of the forebrain and anterior head structures at E8.0. These early prechordal plate defects were transmitted to the underlying neurectoderm leading to loss of *Shh* domains in the ventral forebrain and reduced Hh pathway activation in this tissue. This loss of *Shh* resulted in increased cell death in the ventral neurectoderm and facial ectoderm via the intrinsic apoptotic pathway involving cleaved-caspase 9 and cleaved-caspase 3. Surprisingly, reducing *Ptch1* gene dosage rescued the apoptosis and resulting midface defect. Our results have uncovered a new role for the transition zone complex in mediating signaling crosstalk from the prechordal plate to the neurectoderm to coordinate forebrain and midface development. We have also identified a new target for the treatment/prevention of ciliopathy-associated midface defects in *Ptch1* and provide the first molecular evidence to explain the etiology of forebrain and facial defects in a poorly understood group of ciliopathies.

2.3 Results

Disruption of the MKS transition zone complex results in narrowing of the facial midline

Among the array of craniofacial phenotypes described in ciliopathy patients and observed in transition zone cilia mouse mutants are the presence of midline defects including holoprosencephaly and hypotelorism (Dowdle et al., 2011; Garcia-Gonzalo et al., 2011). However, the developmental origin and molecular etiology for these defects remain poorly characterized. We utilized multiple transition zone mouse models (*Tctn2, Tmem231, Cc2d2a,* and *Tmem67*) to provide a detailed analysis of potential midline facial defects during early craniofacial development. We measured the infranasal distance (distance between the nasal pits, the anlage of the nostrils) to quantify midface width and in *Tctn2* mutant embryos at E10.5 this distance was significantly decreased when compared to heterozygous and wildtype controls (**Figure 1A-C**). One day later at E11.5 the midfacial narrowing persisted and worsened leading to hypoplasia of the frontonasal prominence and fusion of the two maxillary prominences across the midline (**Figure 1E-G**). The midface defect was also evident at E12.5 (**Figure 1I-J**) indicating that an early craniofacial defect persists through the early fusion and growth of the facial primordia during the early stages of craniofacial development. Indeed, the same midline defects were also seen in *Tmem231* and *Cc2d2a* mutants (**Figure 2 and Figure 3**) at similar developmental stages indicating a common origin for the midline facial defects in multiple ciliopathy mouse models. Interestingly, midfacial defects were not seen in *Tmem67* mutants (**Figure 4**) indicating that while some transition zone components are critical for early midfacial development, others are dispensable for this process. This result is consistent with previous reports indicating that while loss of *Tmem67* results in loss of some receptor localization to the

primary cilia (AC3, Arl13b), other receptors critical for normal craniofacial development (Smo) exhibit normal localization (Garcia-Gonzalo et al., 2011).

Defects in prechordal plate signaling precede and drive the development of midface defects in Tctn2 mutants

The presence of midfacial defects at E10.5 suggests that an early signaling defect contributes to the development of this phenotype. In fact, midfacial narrowing was observed in *Tctn2* mutants at E9.5 (data not shown). In an effort to uncover the causative molecular defects that precede the midface defects we focused our analysis on an organizing center critical for forebrain and craniofacial development: the prechordal plate (Kiecker & Niehrs, 2001; Muenke & Beachy, 2000; Rubenstein & Beachy, 1998; Som, Streit, & Naidich, 2014). We focused on this organizing center for three reasons. First, this organizing center is temporally active at a timepoint immediately preceding the phenotypic manifestation of forebrain and midface defect. Second, this tissue has a well-documented role in regulating Hh pathway activation in the forebrain (C. Anderson & Stern, 2016; Aoto et al., 2009; Fuccillo et al., 2006; Rubenstein & Beachy, 1998; Som et al., 2014). Finally, the key finding that surgical removal of this organizing center in rat embryos results in midface collapse that closely resembles the defect seen in transition zone cilia mutants made it an intriguing target for investigation(Aoto et al., 2009). Analysis of transition zone function at the prechordal plate through localization of the ciliary membrane protein Arl13b revealed this localization was severely disrupted in *Tctn2* mutants (**Figure 5A-B**). Is Arl13b ciliary localization disrupted as a result of defects in ciliogenesis in the prechordal plate? Since the transition zone complex is required for proper cilia formation in some tissues but not others we performed gross analysis of ciliogenesis in the prechordal plate

via immunostaining for the ciliary core structural protein acetylated tubulin. Using the prechordal plate marker FoxA2 we found ciliogenesis to be normal in this tissue at E8.0 (**Figure 5E-F**). *In situ* hybridization analysis for axial mesendoderm markers (*Shh, T*) revealed normal expression in both the notochord plate and the prechordal plate (the two contiguous organizing centers which comprise the axial mesendoerm) (**Figure 6A-D**). Normal prechordal plate marker expression suggests the prechordal plate is specified in *Tctn2* mutants. However, expression of the prechordal plate marker *Gsc* was dramatically reduced (**Figure 6E-F**). Since Hh signaling regulates *Gsc* expression in the prechordal plate, we analyzed the output of Hh signaling by examining the expression of the transcriptional target *Gli1*. Indeed, *Gli1* was reduced throughout the axial mesendoderm in *Tctn2* mutants (**Figure 6G-H**). Consistent with signaling defects throughout the axial mesendoderm, expression of the marker *FoxA2* was also reduced (**Figure 6I-J**). Taken together, these results indicate that while induction of the prechordal plate is normal in *Tctn2* mutants, signaling at this organizing center is severely disrupted.

Early prechordal plate defects result in decreased Hh pathway activation and Shh ligand production in the ventral telencephalon

The organizer capacity of the axial mesendoderm has been demonstrated through its ability to induce the adjacent neurectoderm. While the notochord plate is critical for induction of the floor plate at the posterior axis of the neural tube the prechordal plate- located at the anterior-most aspect of the ventral midline- in essential for induction and maintenance of cells in the ventral telencephalon. This is mediated partly through the expression of *Shh* and activation of the Hh pathway in this tissue. As extirpation of the prechordal plate results in decreased *Shh* and Hh pathway activation in the basal telencephalon we investigated whether the prechordal plate

defects seen in *Tctn2* mutants results in similar molecular defects in the ventral telencephalon. While *Shh* in the notochord was normal at E8.5, it was severely reduced in the ventral telencephalon (**Figure 7A-B**). This reduced expression persisted at E9.5 (**Figure 7C-D**). Analysis of Hh pathway activation in this tissue via expression of the transcriptional targets *Gli1* and *Ptch1* revealed that both were severely reduced or absent in the basal forebrain (**Figure 7E-H**). Consistent with the WM-ISH data, qRT-PCR analysis of E8.5 and E9.5 *Tctn2* mutant heads also showed decreased *Shh, Ptch1,* and *Gli1* (**Figure 7I-J**). In sum, these results highlight an early molecular defect in signaling crosstalk from the prechordal plate to the adjacent neurectoderm that presage and contribute to the midface defects in *Tctn2* mutants. These results lead us to investigate what factor(s) may contribute to the loss of *Shh* in the basal forebrain of *Tctn2* mutants. An intriguing potential candidate is the transcription factor Six3: a known regulator of *Shh* in the basal forebrain and transcriptional target of the Hh pathway. WM-ISH experiments (**Figure 7K-L**) showed normal expression of *Six3* in *Tctn2* mutants compared to controls, a result that was further validated via RT-qPCR analysis (**Figure 7M**).

Transition zone dysfunction results in normal proliferation but increased cell death in the neurectoderm and facial ectoderm of Tctn2 mutants

Given the demonstrated role for Shh as a morphogen to induce cell proliferation (D. H. A. J. A. Helms, 1999; Hu et al., 2015) in the developing craniofacial complex as well as evidence that Hh signaling is critical for cell survival (Ahlgren & Bronner-Fraser, 1999; Aoto et al., 2009; Aoto & Trainor, 2015; Litingtung & Chiang, 2000) we measured cell proliferation and cell death in the midface of *Tctn2* mutants. We hypothesized that the reduction in midface width was due to decreased cell proliferation, increased apoptosis, or a combination of both. Analysis of

proliferation using the M-phase cell cycle marker phospho-histone H3 showed normal levels throughout the dorsal-ventral axis of *Tctn2* mutants (**Figure 8B-B"**) compared to controls (**Figure 8A-A"**) as well as in the individual tissue types comprising the craniofacial complex (**Figure 8C**). TUNEL analysis of apoptosis revealed normal/low levels of cell death in dorsal sections of the telencephalon in *Tctn2* mutants compared to controls (**Figure 9A-B**), however, these levels were dramatically increased in more basal/ventral sections of the telencephalon of *Tctn2* mutants (**Figure 9B'-B"**) compared to controls (**Figure 9A'-A"**). Quantification of the percent of TUNEL-positive nuclei in the various tissues that contribute to the craniofacial complex (forebrain, hindbrain, facial ectoderm, and mesenchyme) revealed a significant increase in cell death in the neurectoderm (both in the forebrain and hindbrain) and non-neural ectoderm (facial ectoderm) while levels in the mesenchyme were normal (**Figure 9C**). These data suggest that increased cell death, but not reduced proliferation, in the neurectoderm and non-neural ectoderm triggers the midfacial collapse in *Tctn2* mutants.

Increased cell death in Tctn2 mutants occurs via the cleaved-Caspase 3 and cleaved-Caspase 9 intrinsic apoptotic pathway

We next set out to determine what molecular pathway mediates this increased cell death observed in *Tctn2* mutants. Previous work has shown that the increased cell death observed in both *Shh* null embryos and those where the Hh pathway was inhibited in the forebrain occurred via the intrinsic apoptotic pathway evidenced by increased levels of the central mediators cleaved-Caspase 3 and cleaved-Caspase 9 (Aoto et al., 2009; Aoto & Trainor, 2015). Additional support for this pathway possibly mediating the cell death in transition zone mutants is provided by work showing a non-canonical role for the Ptch1 receptor in directly activating this intrinsic

apoptotic pathway through a DRAL-caspase-9 complex (Mille et al., 2009; Thibert et al., 2003). In support of this pathway contributing to the midface phenotype we found increased cleaved-Caspase 9 and cleaved-Caspase 3 in the basal telencephalon and facial ectoderm of *Tctn2* mutants compared to control embryos at E9.5 (**Figure 10**).

The TZ complex may not be required in the neural crest, telencephalon or facial ectoderm to control midfacial development

Given the near ubiquitous nature of primary cilia, we set out to determine in which tissues of the developing craniofacial complex the transition zone is required to mediate normal midfacial development. Previous work has shown the presence of cilia on cells of the prechordal plate (Sulik et al., 1994), neurectoderm (Brugmann et al., 2010a; Garcia-Gonzalo et al., 2011), facial ectoderm (Brugmann et al., 2010a), and neural crest mesenchyme (Schock et al., 2015), all cell types with demonstrated roles in craniofacial development. Using the cre-loxP system, we conditionally ablated *Tctn2* in the neural crest using the *Wnt1-cre* driver (Danielian, Muccino, Rowitch, Michael, & McMahon, 1998), in the telencephalon/facial ectoderm using the *Foxg1-cre* driver (Hébert & McConnell, 2000), in the facial ectoderm using the *Crect-cre* driver (Forni, Taylor-Burds, Melvin, Williams, & Wray, 2011; Reid et al., 2011), in the prechordal plate using the *Islet1-cre* driver (Harrelson, Kaestner, & Evans, 2012), and in the neurectoderm using the *Sox1-cre* driver. As our previous results suggest an early signaling defect from the prechordal plate to the neurectoderm as the cause for midface collapse we sought to confirm this using a tissue-specific approach using cre drivers that delete in these tissue at timepoints consistent with the observed defect. While recombination of the $R26^{EYFP}$ reporter showed robust activation in the appropriate tissues at the expected embryonic timepoints, *Tctn2* deletion using each of these cre

drivers did not result in the midfacial narrowing seen in *Tctn2* global deletion (**Figure 11-Figure 15**).

Is reporter recombination an accurate readout for loss of Tctn2 function? To address this we used Arl13b ciliary localization as a proxy for Tctn2 function. Loss of Arl13b ciliary localization in the neurectoderm/facial ectoderm and the neural crest at E10.5 using the *Foxg1*-cre (**Figure 15**) and *Wnt1*-cre (**Figure 13**) respectively indicated consistent reporter recombination and loss of Tctn2 function. However, discrepancies were found in early recombination of the mTmG reporter in the prechordal plate and neurectoderm compared to Arl13b ciliary localization. While robust mTmG recombination was observed in the prechordal plate at E8.5 (**Figure 11**) and in the neurectoderm at E9.5 (**Figure 12**), Arl13b ciliary localization persisted at these timepoints in the respective tissues. This raises the possibility that there may be low turnover of Tctn2 protein or that low levels might be sufficient to maintain transition zone function. These results suggest an early role for the TZ complex in coordinating midface development at a timepoint that precedes the activation of current genetic tools used for conditional deletion in the craniofacial complex.

Reducing Ptch1 gene dosage rescues the midface defect in transition zone mutants

Based on our observation that reduced Hh pathway activity in both the prechordal plate and the neurectoderm is associated with the midfacial narrowing of TZ mutants, we sought to modulate the Hh pathway to rescue the midface defects. Potential strategies include reducing levels of negative regulators of the pathway (*Ptch1*, *Gli3*, *Sufu*) or increasing levels of pathway activation (*SmoM2*, *Gli2*, *Shh*). Using the former approach, we found that reducing *Ptch1* gene dosage via the $Ptch1^{tm1Mps}$ allele ($Ptch1^{+/-}$) fully rescues the midface defect in both *Tctn2* and *Cc2d2a* null

mutants at E11.5 (**Figure 16**). In fact, the midfacial width of rescued embryos was significantly increased compared to wildtype and heterozygous control embryos (**Figure 16**). The phenotypic rescue was not due to restoration of Hh pathway activation or *Shh* in the basal telencephalon as both *Gli1* and *Shh* were reduced by WM-ISH in *Tctn2*$^{-/-}$*;Ptch1*$^{+/-}$ rescued embryos as in *Tctn2*$^{-/-}$ mutants *(***Figure 17**). Although apoptosis in the most ventral sections of the telencephalon was observed in *Tctn2*$^{-/-}$*;Ptch1*$^{+/-}$ rescue embryos there was a significant reduction in the amount of cell death in more dorsal sections of the telencephalon (**Figure 17**). This suggests a partial rescue of cell death in the neurectoderm/facial ectoderm is capable of restoring normal midfacial width in TZ mutants.

Figure 1

Loss of transition zone complex component Tctn2 results in collapse/narrowing of the facial midline. Fluorescent frontal view images of *Tctn2* wildtype, heterozygous and null embryos at E10.5 (A-C), E11.5 (E-G) and E12.5 (I-K). Quantification of midface width (denoted by yellow brackets) at respective timepoints was measured by comparing the infranasal distance between embryo samples. For statistical analysis, one-way ANOVA was performed followed by Tukey's multiple comparisons test. Error bars represent the standard deviation and sample size (n) is indicated above error bars. **** $p<0.0001$

Figure 1

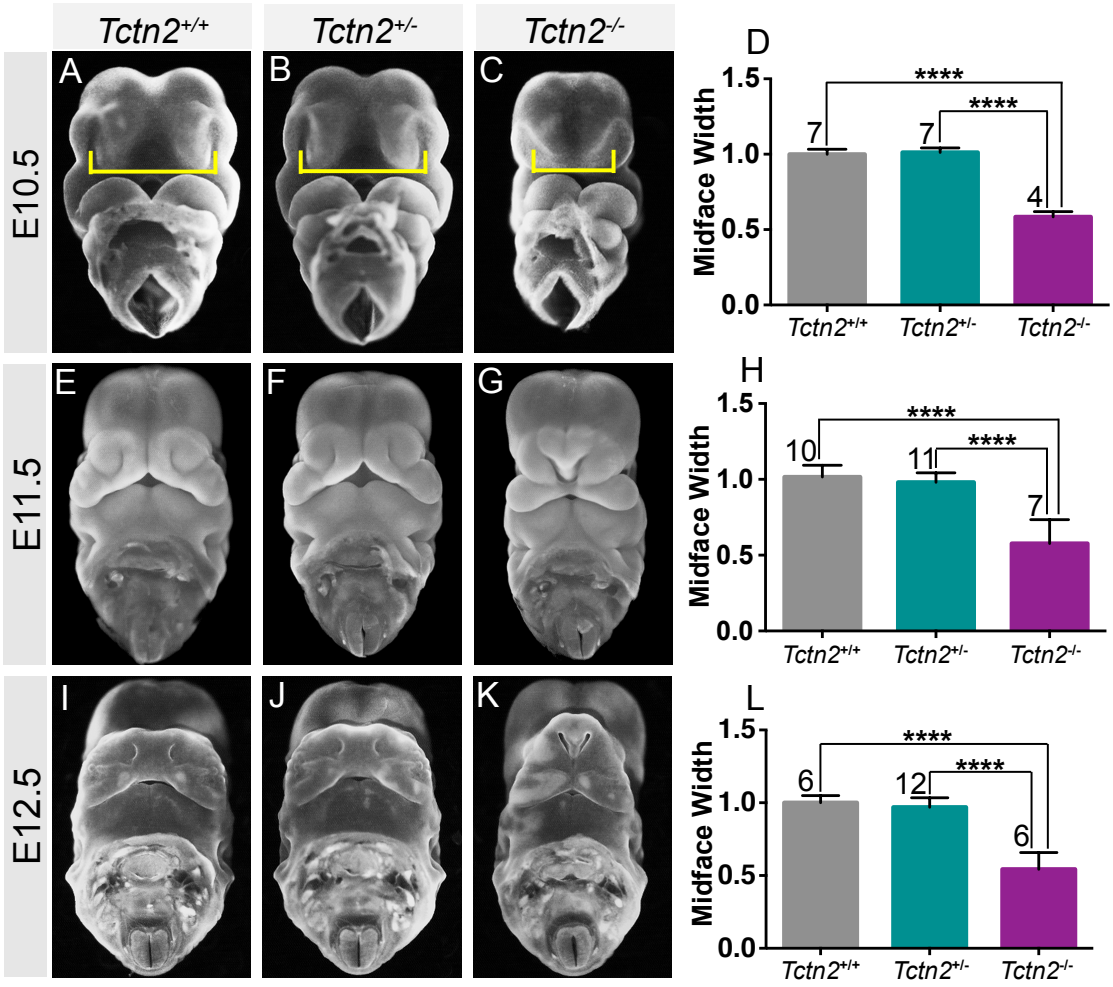
Tctn2+/+
Tctn2+/-
Tctn2-/-
E10.5
E11.5
E12.5
A
B
C
D
E
F
G
H
I
J
K
L
Midface Width
1.5
1.0
0.5
0.0
****
****
7
7
4
10
11
7
6
12
6
Tctn2+/+
Tctn2+/-
Tctn2-/-

Figure 2

Loss of transition zone complex component Cc2d2a results in collapse/narrowing of the facial midline. Fluorescent frontal view images of *Cc2d2a* wildtype, heterozygous and null embryos at E10.5 (A-C) and E11.5 (E-G). Quantification of midface width at respective timepoints (D, H) was measured by comparing the infranasal distance between embryo samples. For statistical analysis, one-way ANOVA was performed followed by Tukey's multiple comparisons test. Error bars represent the standard deviation and sample size (n) is indicated above error bars. **** $p<0.0001$, *** $p<0.0005$

Figure 2

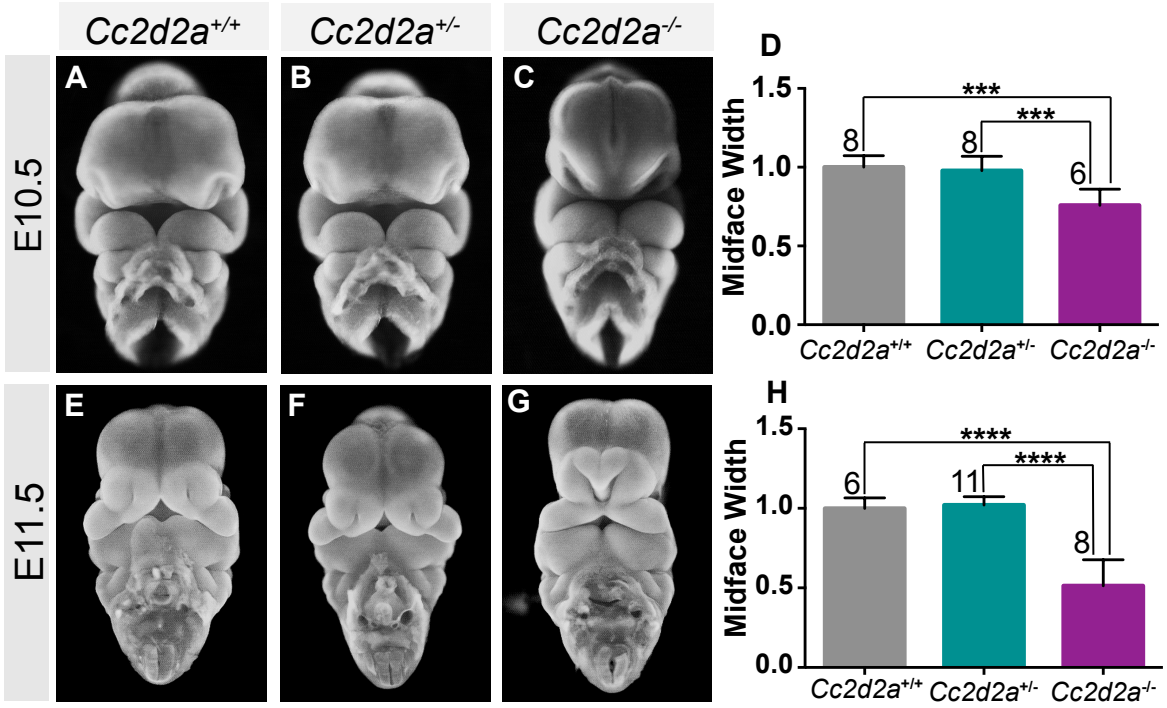
Cc2d2a+/+
Cc2d2a+/-
Cc2d2a-/-
E10.5
E11.5
A
B
C
D
E
F
G
H
Midface Width
1.5
1.0
0.5
0.0
***
***
8
8
6
****
****
6
11
8
Cc2d2a+/+
Cc2d2a+/-
Cc2d2a-/-

Figure 3

Loss of transition zone complex component Tmem231 results in collapse/narrowing of the facial midline. Fluorescent frontal view images of *Tmem231* wildtype, heterozygous and null embryos at E10.5 (A-C) and E11.5 (E-G). Quantification of midface width at respective timepoints (D, H) was measured by comparing the infranasal distance between embryo samples. For statistical analysis, one-way ANOVA was performed followed by Tukey's multiple comparisons test. Error bars represent the standard deviation and sample size (n) is indicated above error bars. *$p<0.05$, ** $p<0.01$

Figure 3

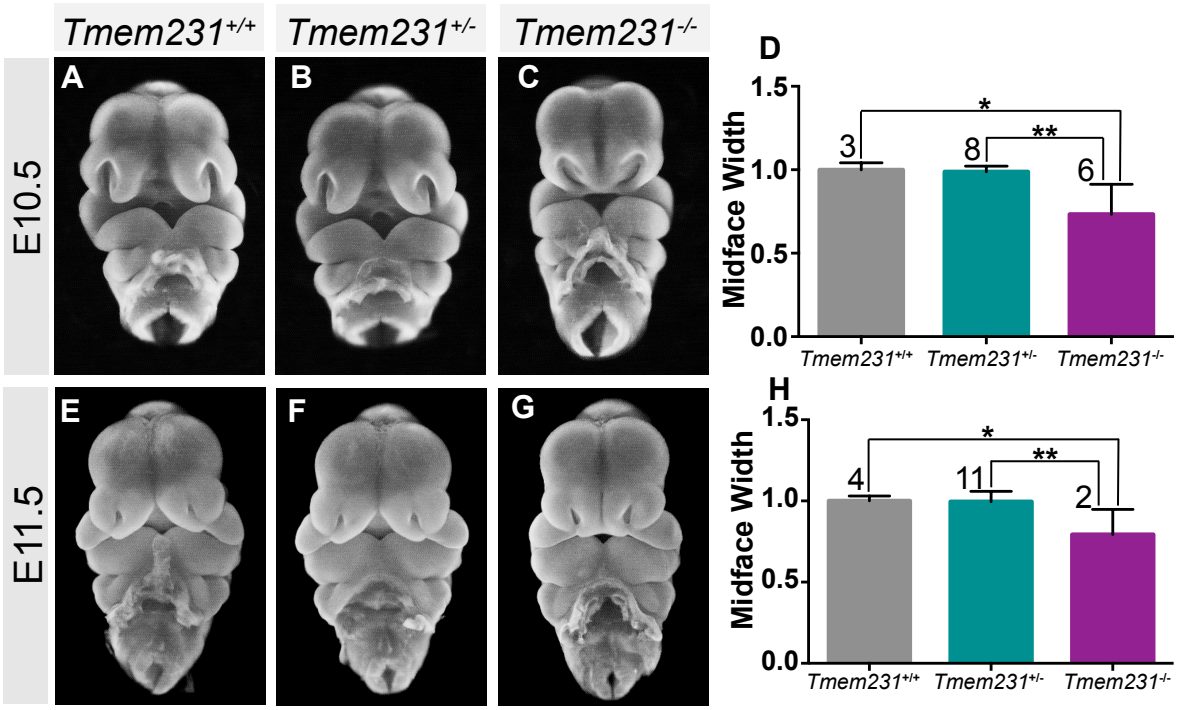
Tmem231+/+
Tmem231+/-
Tmem231-/-
E10.5
E11.5
A
B
C
E
F
G
D
Midface Width
1.5
1.0
0.5
0.0
*
**
3
8
6
Tmem231+/+
Tmem231+/-
Tmem231-/-
H
Midface Width
1.5
1.0
0.5
0.0
*
**
4
11
2
Tmem231+/+
Tmem231+/-
Tmem231-/-

Figure 4

Loss of transition zone complex component Tmem67 does not affect midface development. Fluorescent frontal view images of *Tmem67* wildtype, heterozygous and null embryos at E11.5 (A-C) with corresponding midface width quantification (D). Quantification of midface width was measured by comparing the infranasal distance between embryo samples. For statistical analysis, one-way ANOVA was performed followed by Tukey's multiple comparisons test. Error bars represent the standard deviation and sample size (n) is indicated above error bars.

Figure 4

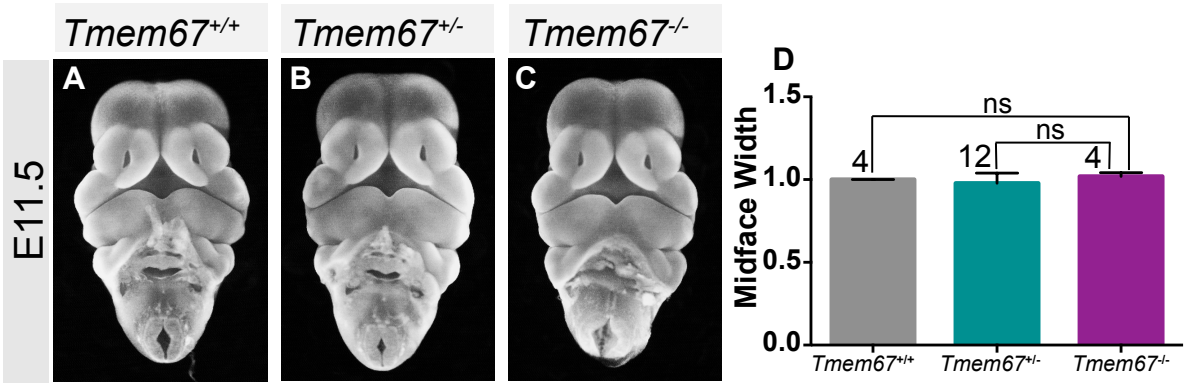
Tmem67+/+
Tmem67+/-
Tmem67-/-
E11.5
A
B
C
D
Midface Width
1.5
1.0
0.5
0.0
ns
ns
4
12
4
Tmem67+/+
Tmem67+/-
Tmem67-/-

Figure 5

Normal ciliogenesis but disrupted Arl13b ciliary localization in the prechordal plate of *Tctn2* mutants. A-B: Whole mount immunofluorecence staining for the ciliary membrane protein Arl13b in E8.0 embryos. C-D: 10uM sagittal section of E8.25 embryos stained for axial mesendoderm marker FoxA2. E-F represents boxed region in C-D rotated 90 degrees clockwise with co-immunostaining for FoxA2, basal body marker gamma-Tubulin, and acetylated tubulin (AcTub).

Figure 5

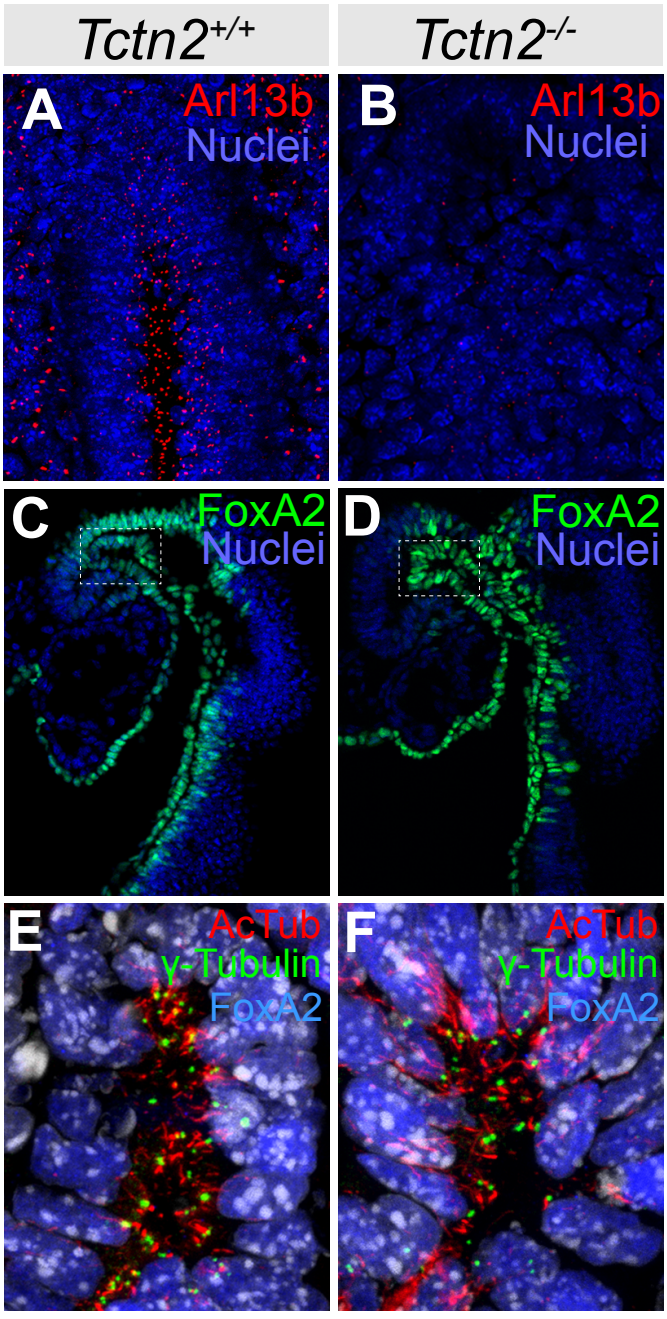
Tctn2+/+
Tctn2-/-
A
Arl13b
Nuclei
B
Arl13b
Nuclei
C
FoxA2
Nuclei
D
FoxA2
Nuclei
E
AcTub
γ-Tubulin
FoxA2
F
AcTub
γ-Tubulin
FoxA2

Figure 6

Loss of Tctn2 results in defects in prechordal plate signaling. Whole mount *in situ* hybridization of E8.0 embryos for axial mesendoderm markers *Shh* and *T* (A-D) reveal normal expression in *Tctn2* mutants indicating normal induction of the prechordal plate. Decreased expression of prechordal plate-specific marker *Gsc* (E-F), Hh pathway transcriptional target *Gli1* (G-H) and endoderm-specifying transcription factor *FoxA2* (I-J) indicates signaling defects in the prechordal plate. Box in E-F highlights prechordal plate region and line in G-H outlines the axial mesendoderm.

Figure 6

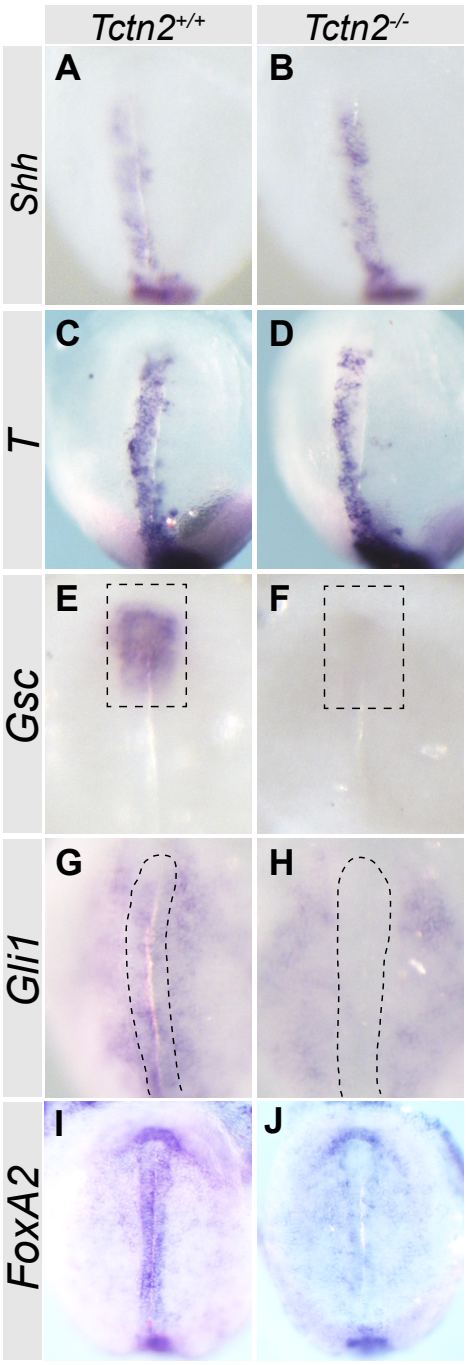

Figure 7

Early prechordal plate defects result in decreased Hh pathway activation and *Shh* expression in the ventral telencephalon. WM-ISH for *Shh* in *Tctn2* controls and mutants at E8.5 (A-B) and E9.5 (C-D) shows reduced expression in the ventral telencephalon of mutant embryos (arrowheads). WM-ISH for Hh pathway targets *Ptch1* (E-F) and *Gli1* (G-H) also show reduced expression in the ventral telencephalon in *Tctn2* mutants (arrowheads). RT-qPCR analysis of RNA transcripts isolated from E8.5 and E9.5 *Tctn2* control and mutant heads (I and J respectively) show reduced levels of *Shh*, *Gli* and *Ptch1* transcripts, consistent with WM-ISH results. Expression of the transcription factor *Six3*- a known regulator of *Shh* in the basal forebrain- is unchanged in *Tctn2* mutants (L) compared to controls (K) at E8.5. RT-qPCR analysis confirms normal levels of *Six3* in mutant embryos (M). * $p<0.05$, ** $p<0.01$, *** $p<0.001$

Figure 7

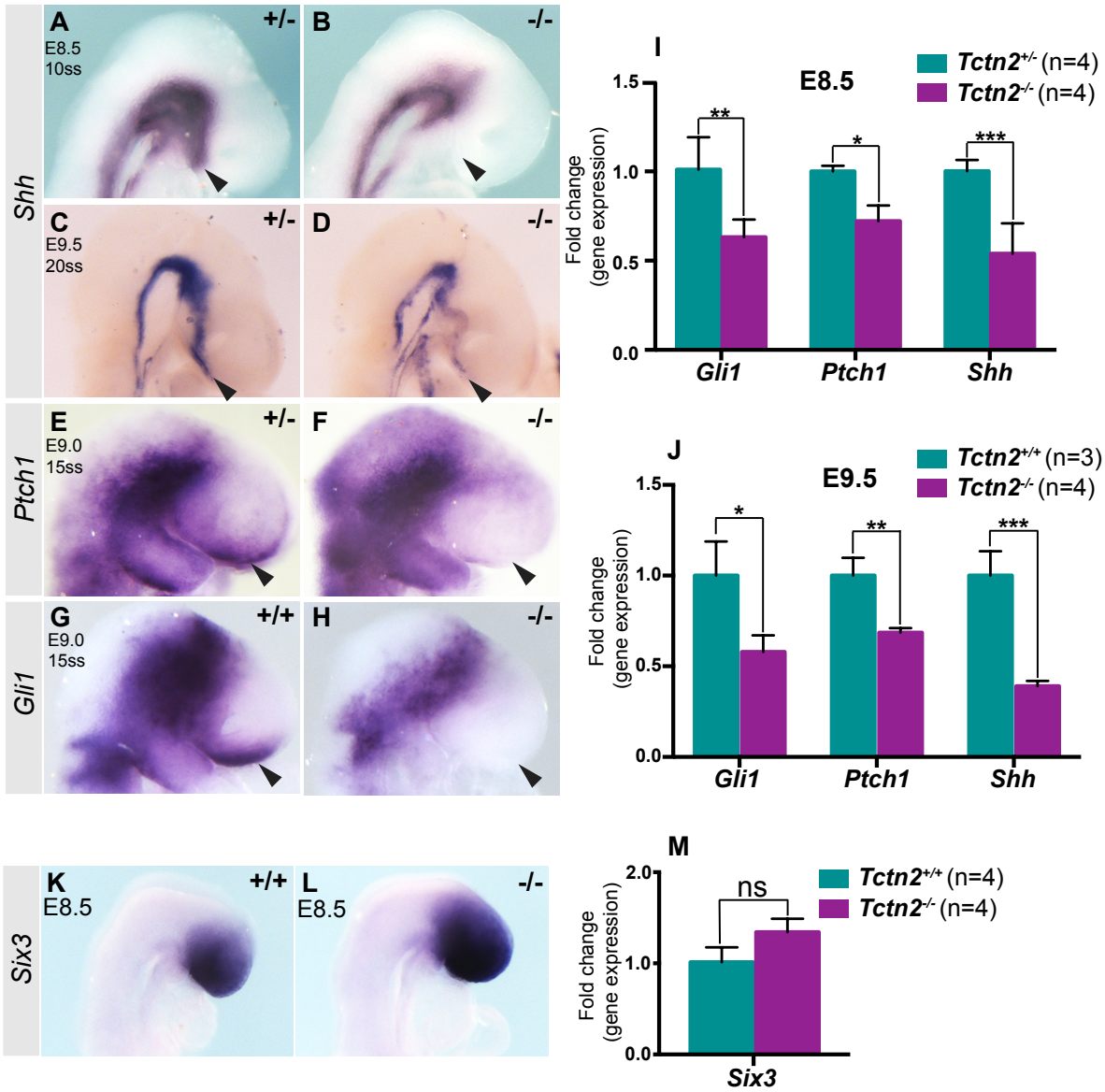
Shh
A
E8.5
10ss
+/-
B
-/-
C
E9.5
20ss
+/-
D
-/-
Ptch1
E
E9.0
15ss
+/-
F
-/-
Gli1
G
E9.0
15ss
+/+
H
-/-
Six3
K
E8.5
+/+
L
E8.5
-/-
I
E8.5
Tctn2+/- (n=4)
Tctn2-/- (n=4)
Fold change
(gene expression)
1.5
1.0
0.5
0.0
**
*
***
Gli1
Ptch1
Shh
J
E9.5
Tctn2+/+ (n=3)
Tctn2-/- (n=4)
Fold change
(gene expression)
1.5
1.0
0.5
0.0
*
**
***
Gli1
Ptch1
Shh
M
Tctn2+/+ (n=4)
Tctn2-/- (n=4)
Fold change
(gene expression)
2.0
1.0
0.0
ns
Six3

Figure 8

Proliferation rates are normal in the craniofacial tissues of *Tctn2* mutants at E9.5. Immunofluorescence staining of proliferation marker phospho-histone H3 (pHH3) in transverse sections of *Tctn2* control (A-A") and mutant (B-B") embryos. C: Quantification of proliferation rates in various tissues of the craniofacial complex in samples from A-B". Note: approximate location of sections in A-A" are depicted in illustration in upper left panel with A' and A" representing successively basal sections.

Figure 8

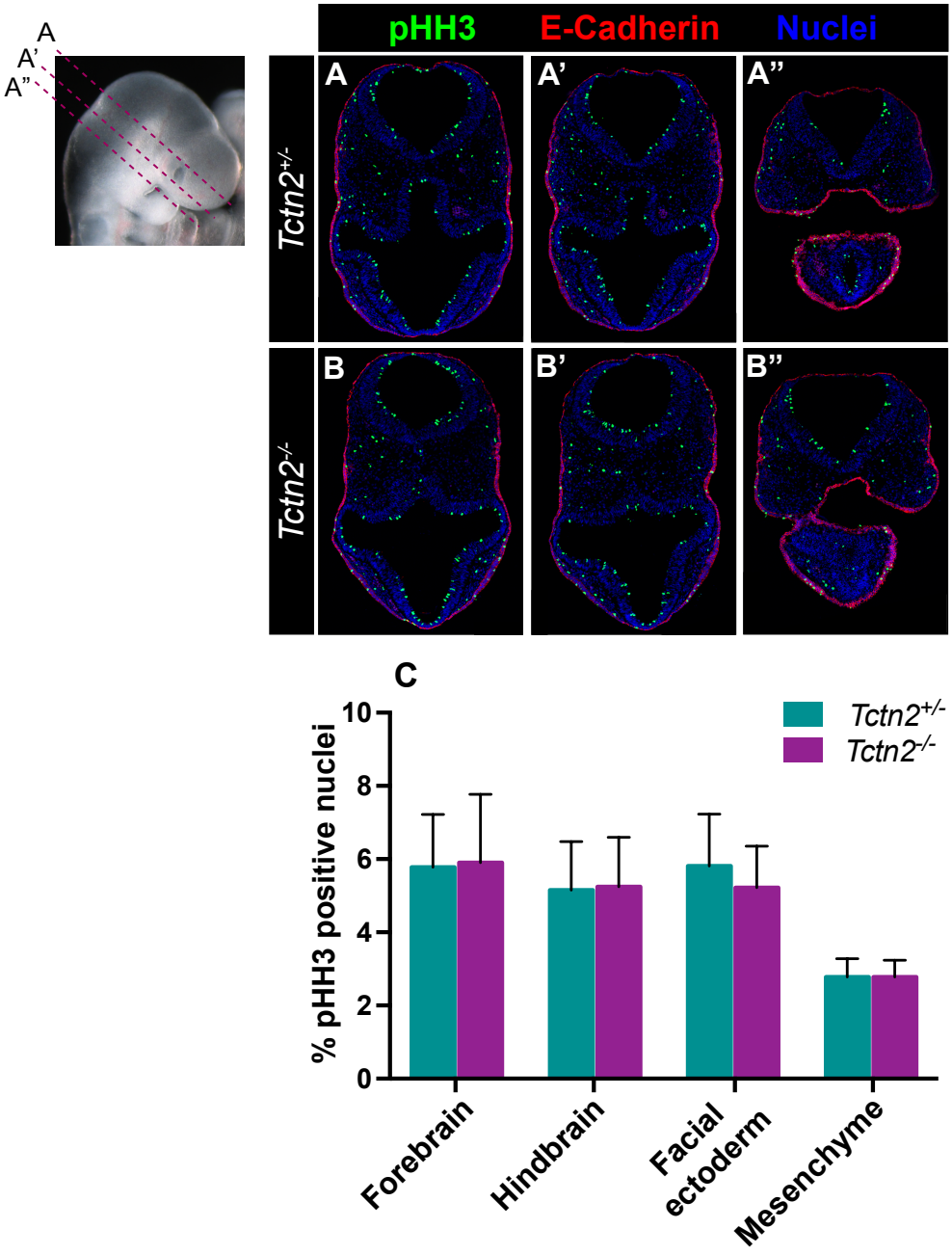
A
A'
A"
pHH3
E-Cadherin
Nuclei
Tctn2+/-
Tctn2-/-
A
A'
A"
B
B'
B"
C
% pHH3 positive nuclei
10
8
6
4
2
0
Tctn2+/-
Tctn2-/-
Forebrain
Hindbrain
Facial ectoderm
Mesenchyme

Figure 9

Increased cell death in the neurectoderm and facial ectoderm drives midface collapse in *Tctn2* mutants. TUNEL assay for analysis of apoptosis in transverse sections of E9.5 control (A-A") and mutant (B-B") embryos. Region of embryo that sections in A-B" were taken indicated in upper left schematic. (C) Represents the quantification of apoptosis in A-B", error bars represent standard deviation. * $p<0.05$, ** $p<0.01$, **** $p<0.0001$

Figure 9

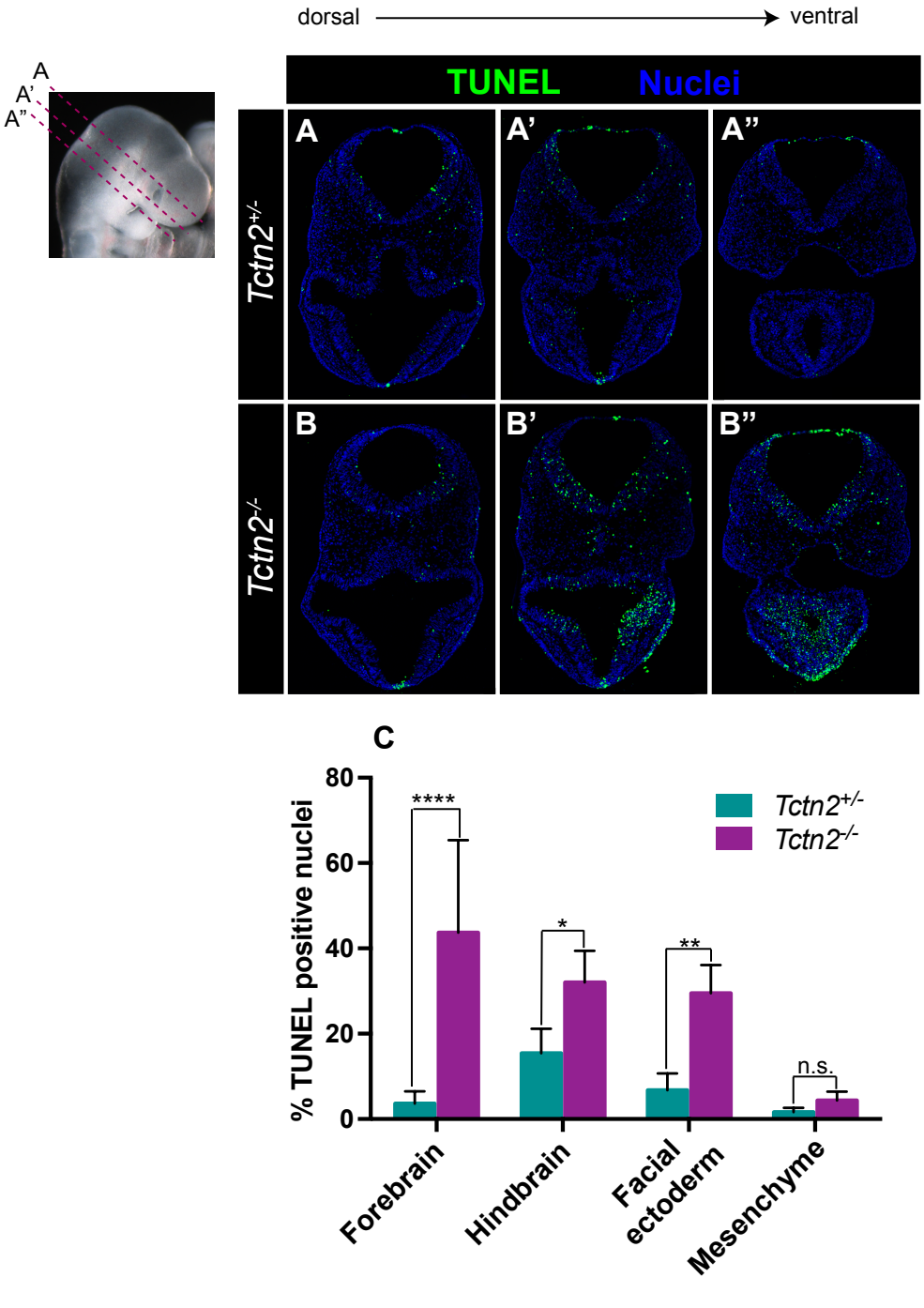
dorsal
ventral
A
A'
A"
TUNEL
Nuclei
Tctn2+/-
Tctn2-/-
A
A'
A"
B
B'
B"
C
% TUNEL positive nuclei
80
60
40
20
0
****
*
**
n.s.
Tctn2+/-
Tctn2-/-
Forebrain
Hindbrain
Facial ectoderm
Mesenchyme

Figure 10

Increased cell death in *Tctn2* mutants occurs via a Caspase-3/Caspase-9 dependent mechanism. 10uM transverse sections immunostained for the central apoptotic pathway component cleaved-Caspase 3 (A,C) or the intrinsic apoptotic protein cleaved-Caspase 9 (B,D) in E9.5 *Tctn2* embryos. Non-specific staining circled in white.

Figure 10

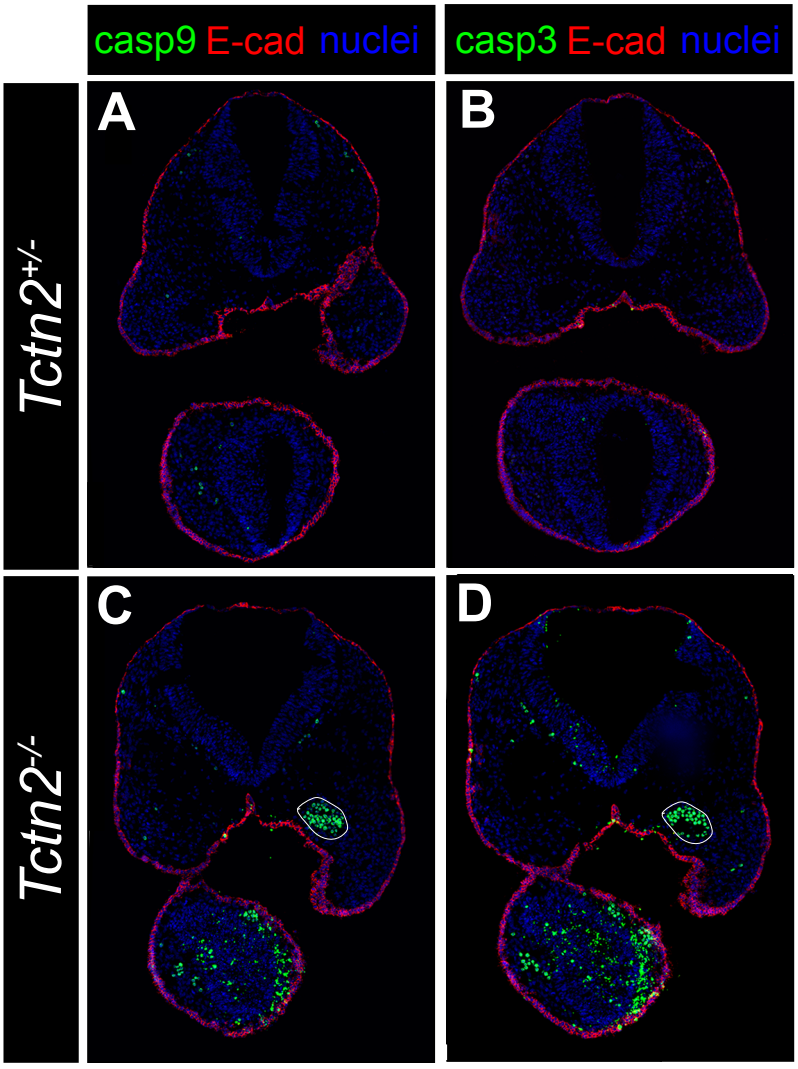

Figure 11

Use of the *Islet1-cre* driver for prechordal plate deletion of Tctn2 function does not result in midface narrowing. (A) Fluorescent frontal images of mutant and control embryos at E11.5 with corresponding midface quantification in (B). Analysis of *Isl1-cre* recombination pattern confirms expected activity in the prechordal plate and endodermal derivatives at E8.5 and E11.5 (C). Analysis into loss of Tctn2 activity using this reporter via Arl13b ciliary localization indicates that while reporter recombination is robust in the prechordal plate at E8.5, Tctn2 function persists in this tissue as Arl13b ciliary localization is normal in mutant embryos (D). Error bars in (B) represent the standard deviation and sample size is indicated above each bar.

Figure 11

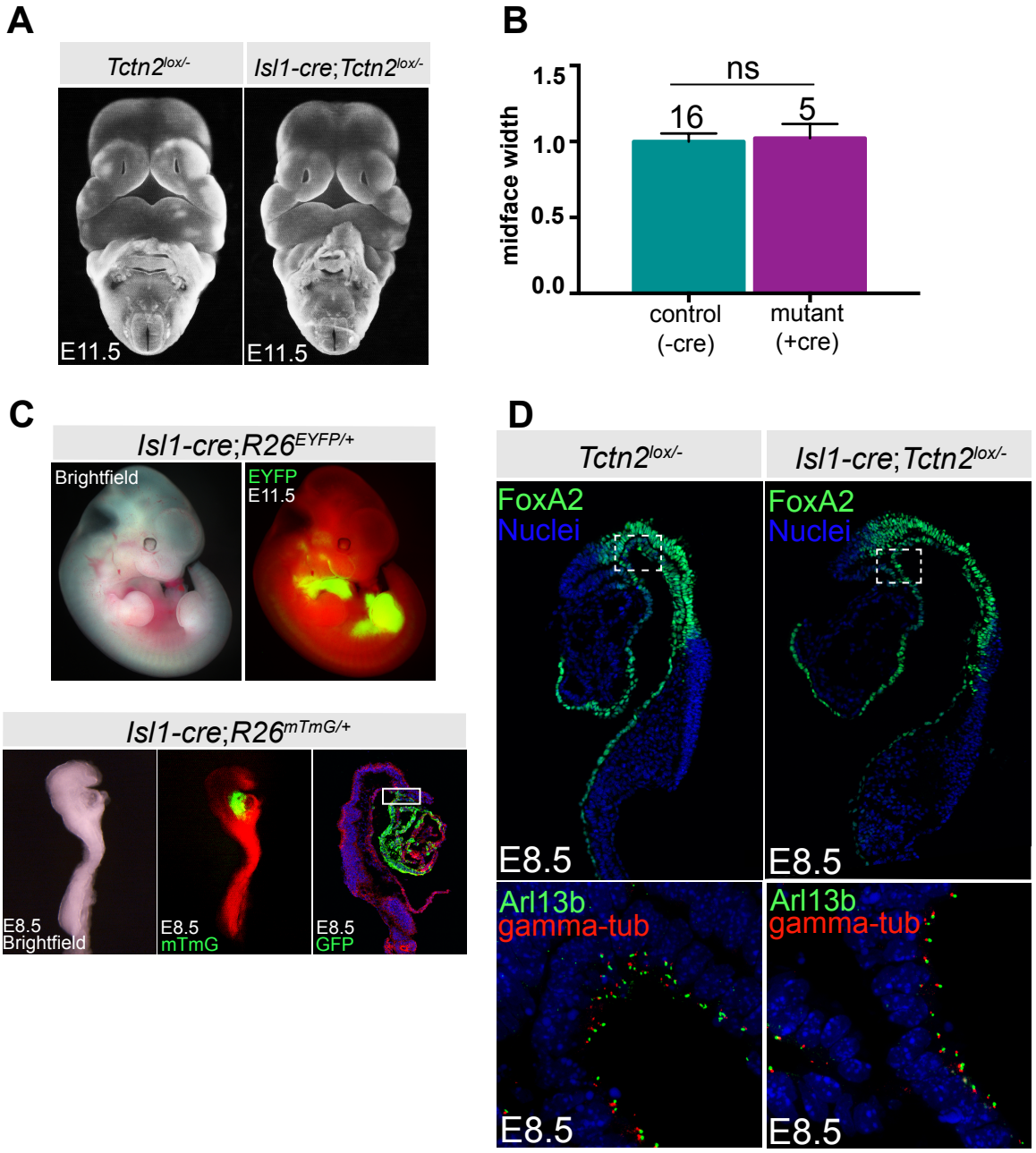
A
Tctn2lox/-
Isl1-cre;Tctn2lox/-
E11.5
E11.5
B
ns
16
5
midface width
1.5
1.0
0.5
0.0
control
(-cre)
mutant
(+cre)
C
Isl1-cre;R26EYFP/+
Brightfield
EYFP
E11.5
Isl1-cre;R26mTmG/+
E8.5
Brightfield
E8.5
mTmG
E8.5
GFP
D
Tctn2lox/-
Isl1-cre;Tctn2lox/-
FoxA2
Nuclei
FoxA2
Nuclei
E8.5
E8.5
Arl13b
gamma-tub
Arl13b
gamma-tub
E8.5
E8.5

Figure 12

Deletion of Tctn2 function in the neurectoderm using the *Sox1-cre* driver does not result in midface narrowing. Fluorescent frontal images of mutant and control embryos (A) and corresponding midface width quantification (B). mTmG reporter recombination shows expected recombination beginning in the neural folds at E8.5 and robust recombination in the neurectoderm at E9.5 and E11.5 (C). Analysis of Tctn2 function via Arl13b ciliary localization shows that while the *Sox1-cre* driver is highly active at E9.5 (C), Arl13b ciliary localization in mutant embryos persists at similar levels to control embryos (D). Error bars in (B) represent the standard deviation and number above error bar indicates sample size. Box in (C) highlights GFP+ cells in the prechordal plate indicating cre-recombination in this tissue type.

Figure 12

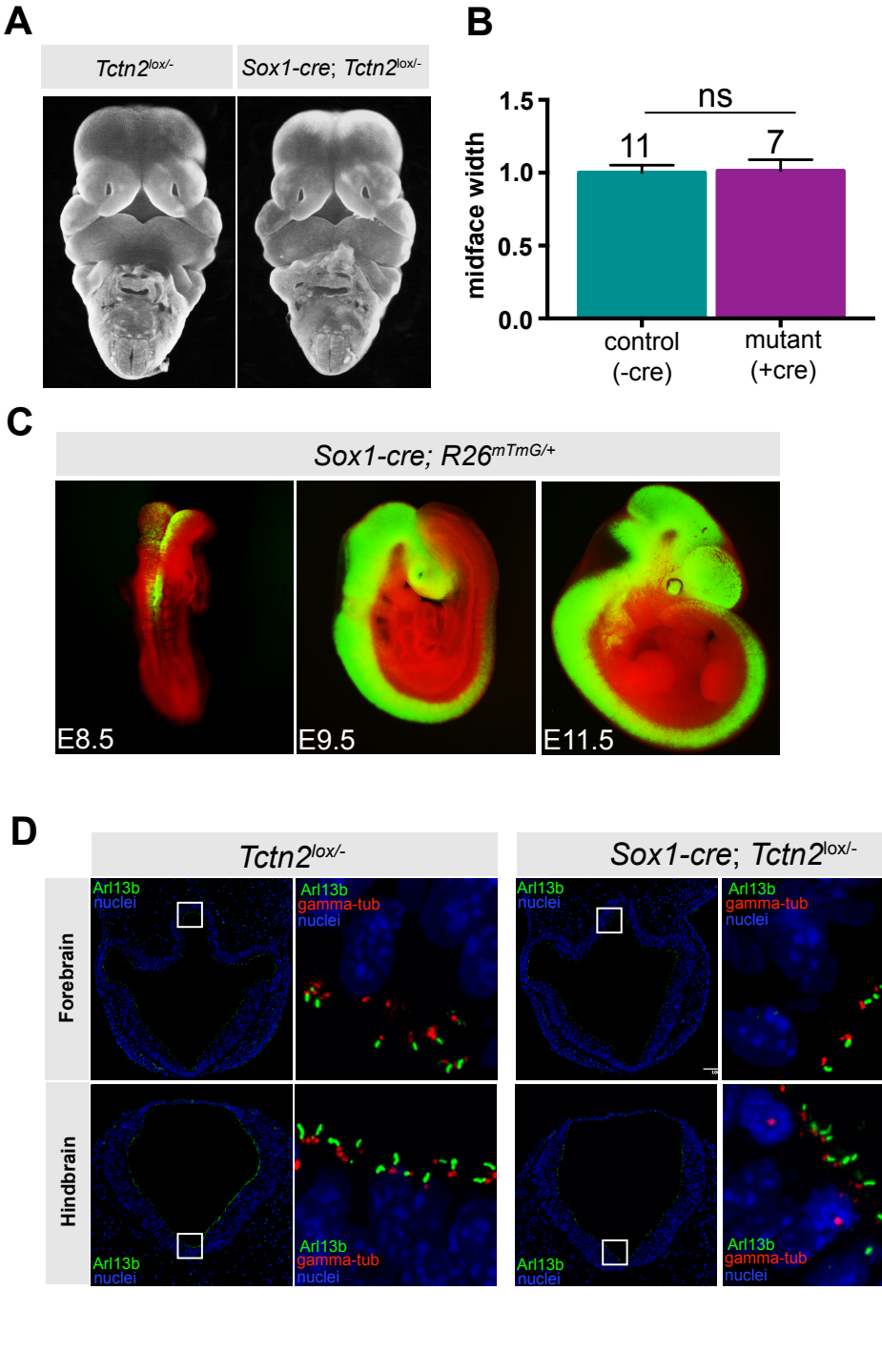
A
Tctn2lox/-
Sox1-cre; Tctn2lox/-
B
ns
11
7
midface width
1.5
1.0
0.5
0.0
control
(-cre)
mutant
(+cre)
C
Sox1-cre; R26mTmG/+
E8.5
E9.5
E11.5
D
Tctn2lox/-
Sox1-cre; Tctn2lox/-
Forebrain
Hindbrain
Arl13b
nuclei
gamma-tub

Figure 13

Deletion of Tctn2 in the neural crest using the *Wnt1-cre* driver does not result in midface narrowing. (A) Fluorescent frontal images of E11.5 *Tctn2* mutant and wildtype embryos and corresponding midface quantification in (B). (C) Confirmation of *Wnt1-cre* reporter recombination in E11.5 embryos show expected pattern for neural crest recombination. (D) Immunofluoresence staining of E10.5 frozen sections through the medial nasal prominence. (D) Loss of Tctn2 function confirmed in the neural crest via loss of Arl13b ciliary localization specifically in the GFP+ neural crest but not in the adjacent facial ectoderm co-stained with epithelial marker E-cadherin (E-cad). Error bars in (B) represent the standard deviation and sample size is indicated above bars.

Figure 13

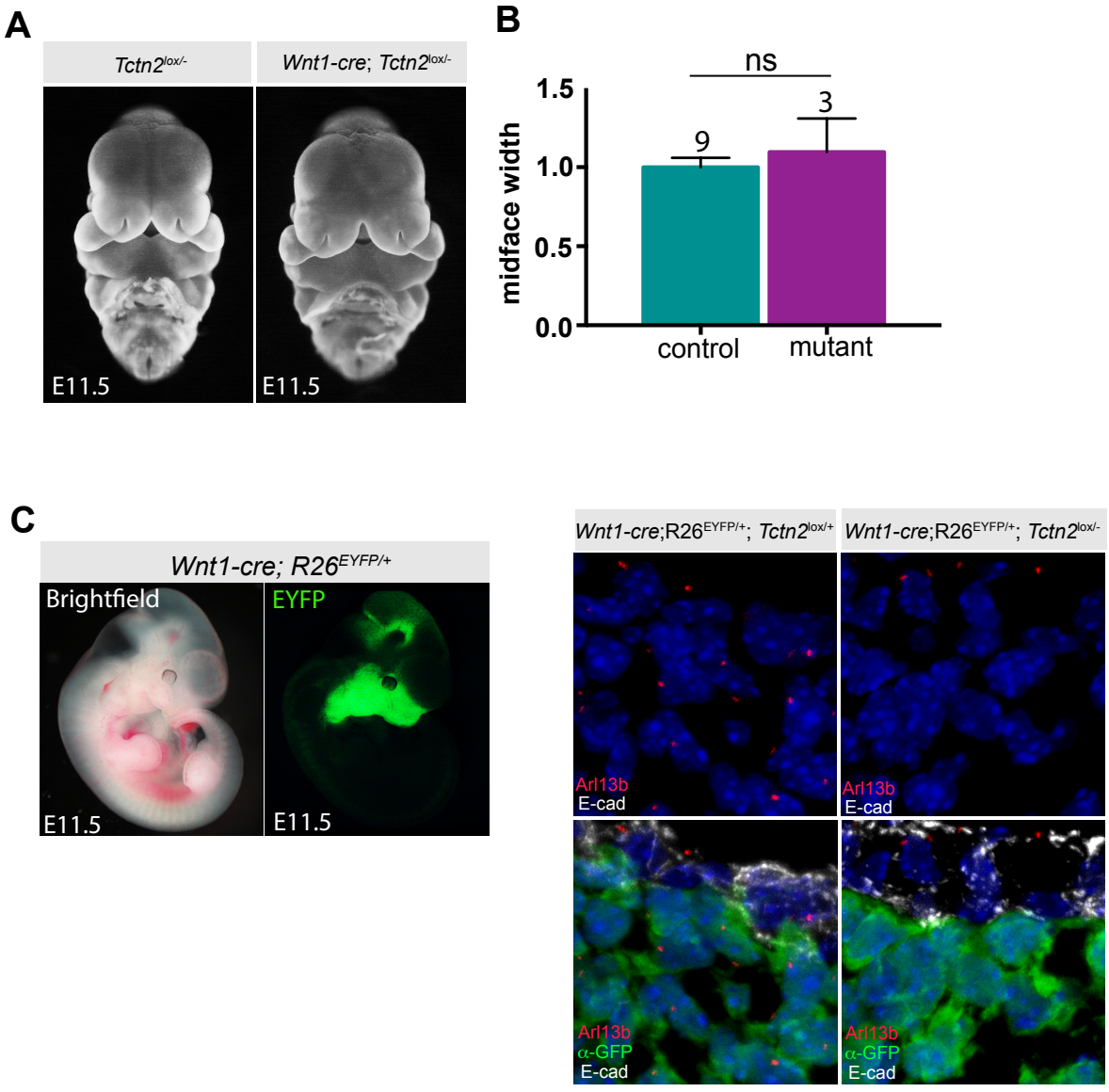
A
Tctn2lox/-
Wnt1-cre; Tctn2lox/-
E11.5
E11.5
B
ns
9
3
1.5
1.0
0.5
0.0
midface width
control
mutant
C
Wnt1-cre; R26EYFP/+
Brightfield
EYFP
E11.5
E11.5
Wnt1-cre;R26EYFP/+; Tctn2lox/+
Wnt1-cre;R26EYFP/+; Tctn2lox/-
Arl13b
E-cad
Arl13b
E-cad
Arl13b
α-GFP
E-cad
Arl13b
α-GFP
E-cad

Figure 14

Deletion of Tctn2 in the facial ectoderm using the *Crect-cre* driver does not result in midface narrowing. (A) Fluorescent frontal images of E11.5 mutant and control embryos with corresponding midface measurements in (B). (C) Analysis of *Crect-cre* recombination pattern at E11.5 shows robust recombination in the facial ectoderm as evidenced by co-staining with epithelial marker E-cadherin. (D) Analysis of Arl13b ciliary localization in mutant and control embryos show decreased localization in mutant embryos but not a complete absence. This indicates possible residual Tctn2 activity remains in cre-recombined tissue at this embryonic timepoint. Error bars in (B) represents the standard deviation and sample size is indicated above error bars.

Figure 14

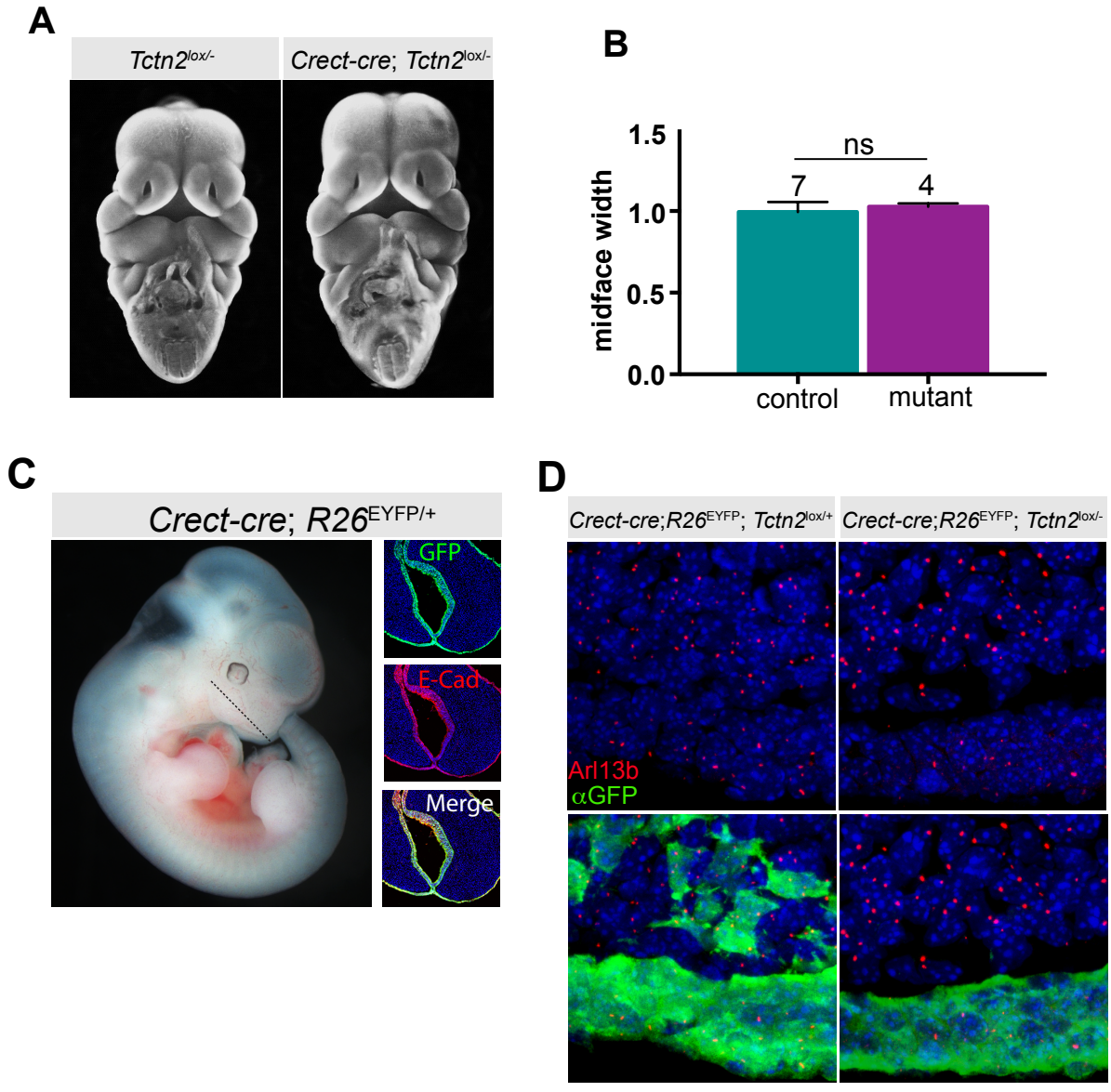
A
Tctn2lox/-
Crect-cre; Tctn2lox/-
B
midface width
1.5
1.0
0.5
0.0
ns
7
4
control
mutant
C
Crect-cre; R26EYFP/+
GFP
E-Cad
Merge
D
Crect-cre;R26EYFP; Tctn2lox/+
Crect-cre;R26EYFP; Tctn2lox/-
Arl13b
αGFP

Figure 15

Deletion of Tctn2 in the forebrain and facial ectoderm using the *Foxg1-cre* driver does not result in midface narrowing. (A) Fluorescent frontal images of E11.5 mutant and control embryos with corresponding midface quantification in (B). (C) Analysis of reporter recombination using the fluorescent reporter *R26EYP* confirms cre-mediated recombination in the expected tissues. (D) Immunofluorescence staining of E11.5 neural tube sections for ciliary protein Arl13b and basal body marker gamma tubulin confirms loss of Tctn2 function in the GFP+ cre-recombined tissue via loss of Arl13b in mutant samples.

Figure 15

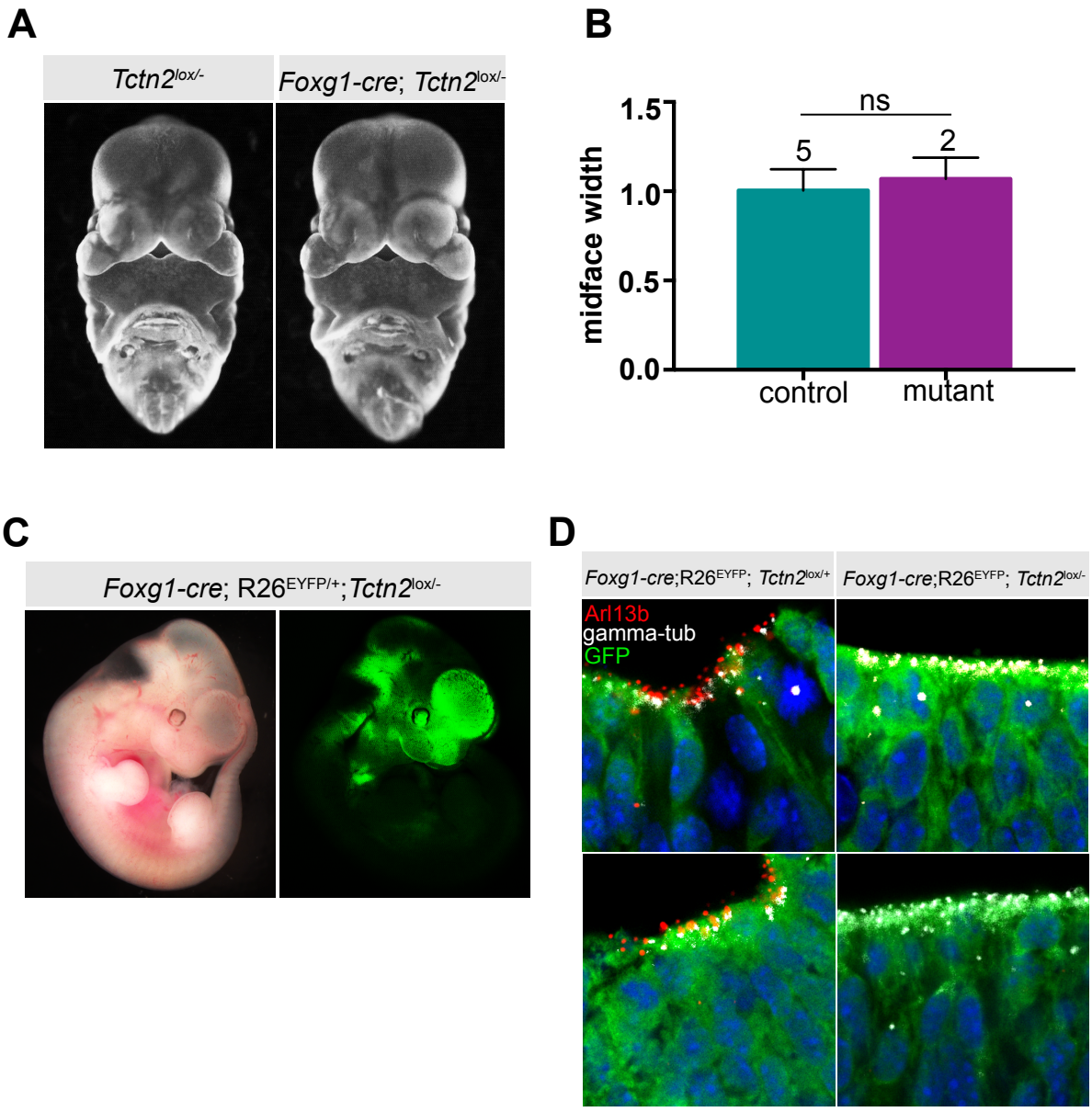
A
Tctn2lox/-
Foxg1-cre; Tctn2lox/-
B
midface width
1.5
1.0
0.5
0.0
ns
5
2
control
mutant
C
Foxg1-cre; R26EYFP/+;Tctn2lox/-
D
Foxg1-cre;R26EYFP; Tctn2lox/+
Foxg1-cre;R26EYFP; Tctn2lox/-
Arl13b
gamma-tub
GFP

Figure 16

Reducing *Ptch1* gene dosage rescues midface collapse in transition zone mutants. (A-C) Fluorescent frontal images of wildtype (A), mutant (B) and rescue (C) E11.5 *Tctn2* embryos with corresponding midface width quantification (D). (E-G) Frontal images of wildtype (E), mutant (F), and rescue (G) E11.5 *Cc2d2a* embryos with corresponding midface width quantification (H). Error bars in (D) and (H) represents the standard deviation. For statistical analysis one-way ANOVA was performed with Tukey's multiple comparison test. **** $p<0.0001$

Figure 16

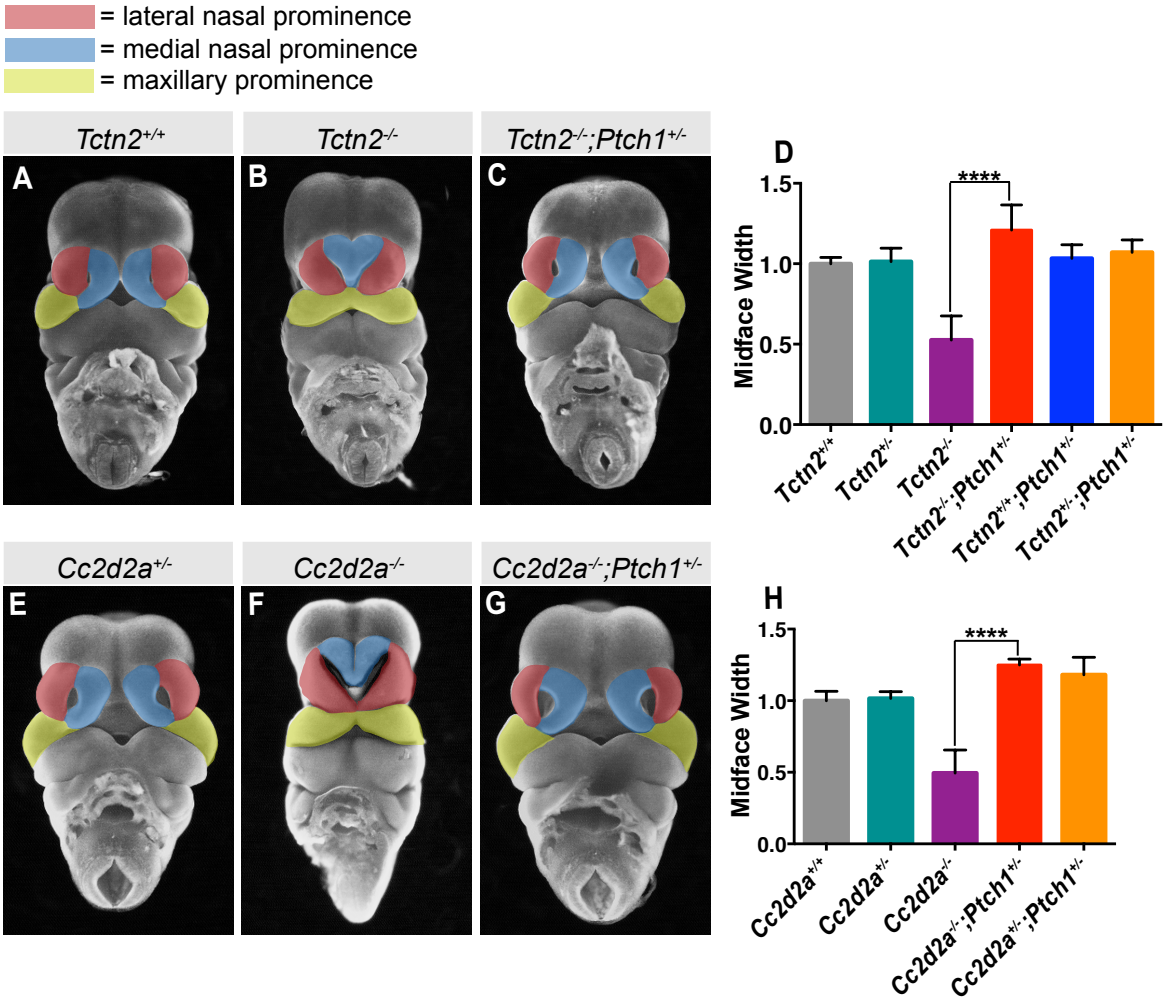
= lateral nasal prominence
= medial nasal prominence
= maxillary prominence
Tctn2+/+
Tctn2-/-
Tctn2-/-;Ptch1+/-
A
B
C
D
Midface Width
1.5
1.0
0.5
0.0
****
Tctn2+/+
Tctn2+/-
Tctn2-/-
Tctn2-/-;Ptch1+/-
Tctn2+/+;Ptch1+/-
Tctn2+/-;Ptch1+/-
Cc2d2a+/-
Cc2d2a-/-
Cc2d2a-/-;Ptch1+/-
E
F
G
H
Midface Width
1.5
1.0
0.5
0.0
****
Cc2d2a+/+
Cc2d2a+/-
Cc2d2a-/-
Cc2d2a-/-;Ptch1+/-
Cc2d2a+/-;Ptch1+/-

Figure 17

Decreased cell death in *Tctn2* mutant embryos with reduced *Ptch1* gene dosage results in normal midface development despite persistent loss of *Shh* and *Gli1* in the basal forebrain. Analysis of cell death via TUNEL assay in control (A-A”), mutant (B-B”) and Ptch1 rescue (C-C”) E9.5 *Tctn2* embryo sections. Image in upper left corner shows approximate region of embryo sections for A-C”. WM-ISH analysis for *Shh* (D-F) and *Gli1* (G-I) in E9.0 control, mutant and *Ptch1* rescue embryos.

Figure 17

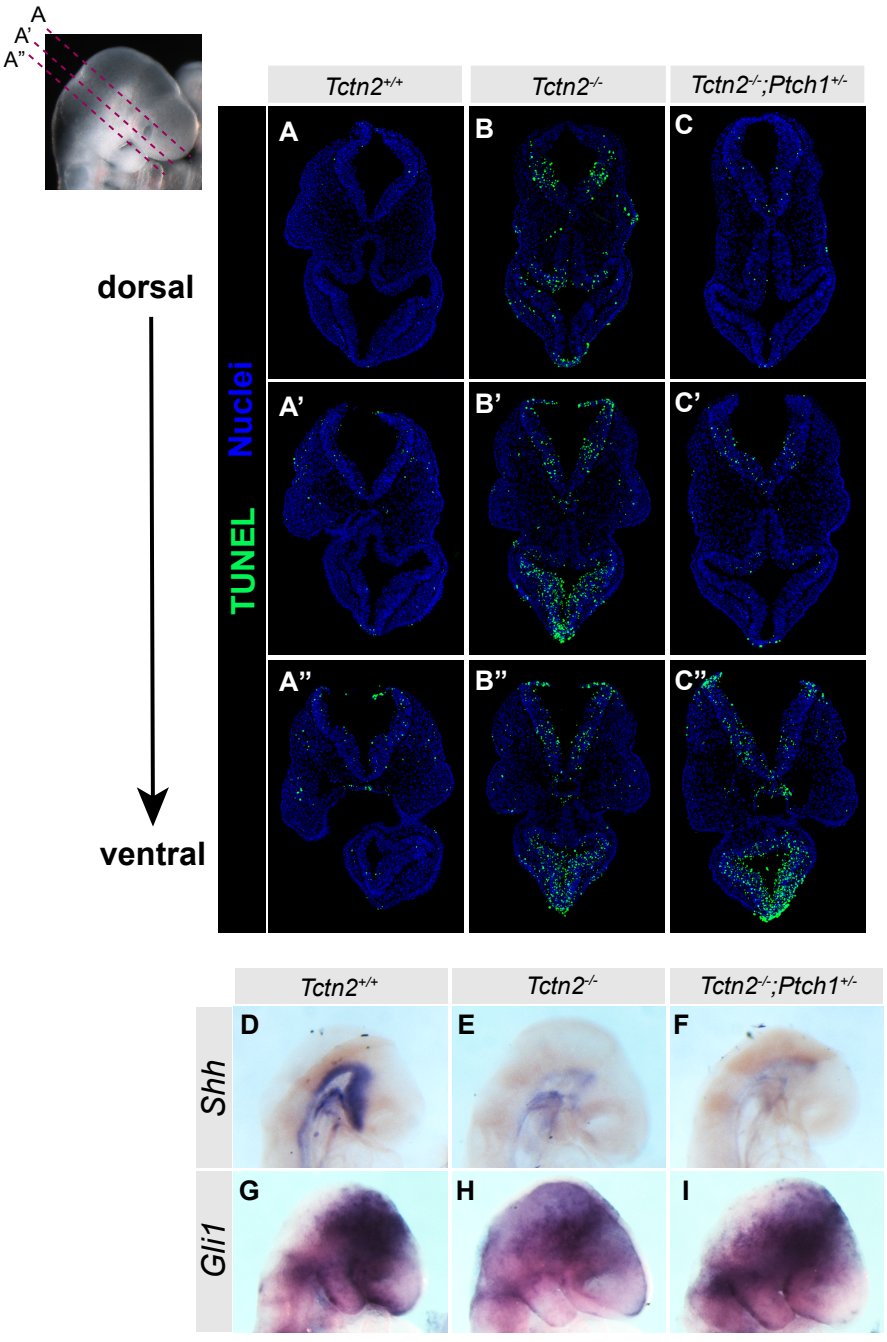
A
A'
A"
dorsal
ventral
Tctn2+/+
Tctn2-/-
Tctn2-/-;Ptch1+/-
TUNEL
Nuclei
A
B
C
A'
B'
C'
A"
B"
C"
Shh
Gli1
D
E
F
G
H
I

Figure 18

Model for TZ coordination of midfacial development. **(A)** In normal embryos, the transition zone complex mediates autocrine signaling in the prechordal plate and signal crosstalk to the adjacent neurectoderm to at allow for cell survival and normal midface development. **(B)** In transition zone mutants loss of signaling in the prechordal plate results in reduced *Shh* and Hh pathway activation in the neurectoderm resulting in massive cell death and corresponding midface collapse. **(C)** In rescue of TZ mutant via decreased *Ptch1* gene dosage, reduced cell death allows for normal midface development despite persistent reduction in *Shh* and Hh pathway activation in the neurectoderm.

Figure 18

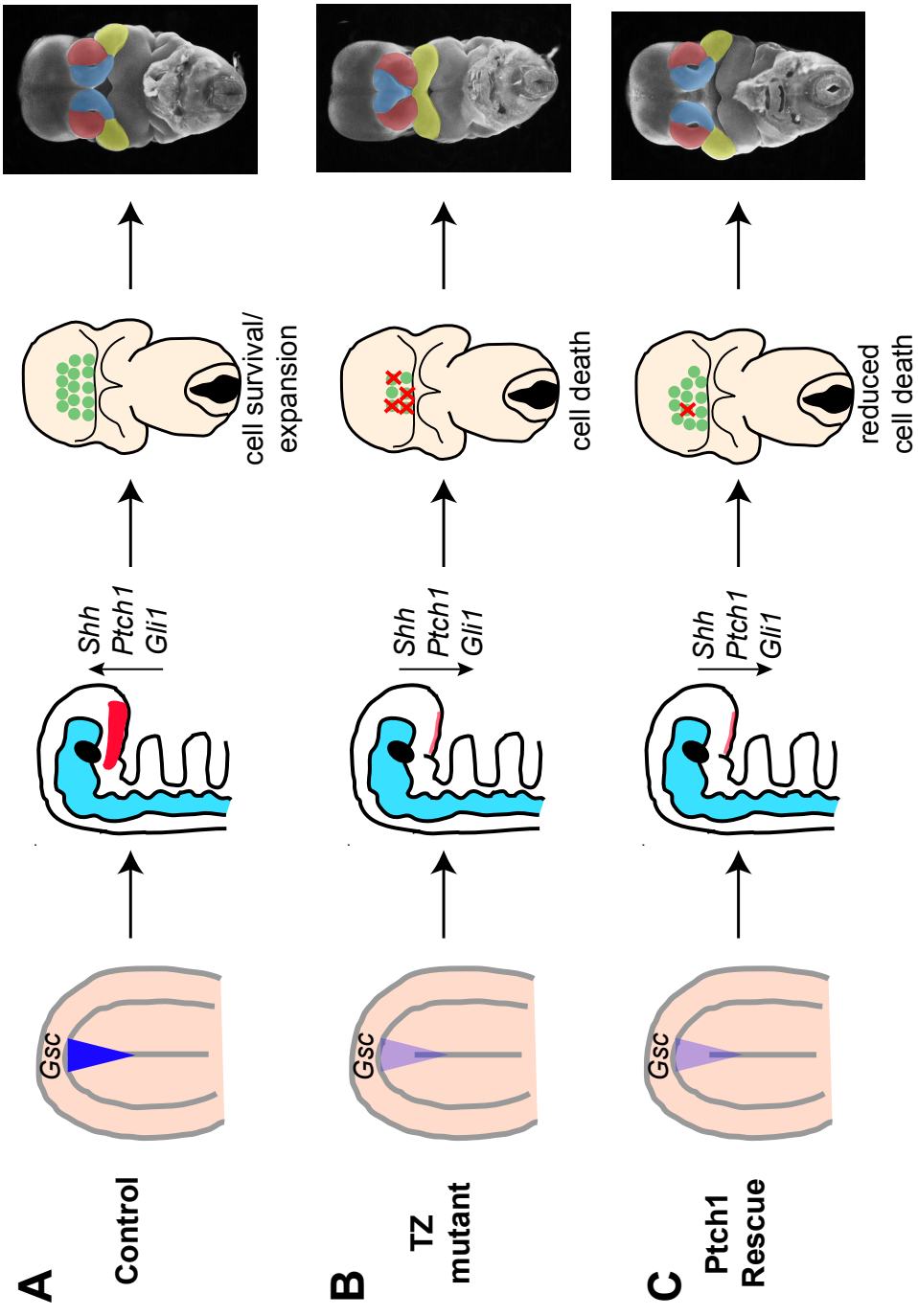
A
Control
B
TZ
mutant
C
Ptch1
Rescue
Gsc
Shh
Ptch1
Gli1
cell survival/
expansion
cell death
reduced
cell death

2.4 Discussion

A topic of confusion among ciliary biologists has been the finding that defects in cilia structure and/or function can in many instances lead to seemingly opposing phenotypes. In the case of ciliary defects that result in midface abnormalities, narrowing and expansion of the midface (hypotelorism and hypertelorism respectively) have both been described as ciliopathy phenotypes (Schock et al., 2015; Zaghloul & Brugmann, 2011). While a ciliary role for Gli3 repressor in controlling the proliferation of neural crest cells has been described in the etiology for midface expansion, our mechanistic understanding for the cause of midface narrowing is currently poorly understood (Brugmann et al., 2010a; Chang et al., 2014; Liu et al., 2014). This work provides the first experimental evidence for the molecular underpinnings leading to midface hypoplasia caused by defects in the ciliary transition zone protein complex.

In order to uncover the source of a developmental defect it is critical to look in the right place at the right time. A key finding in this study is the identification of prechordal plate signaling defects as the earliest molecular defect that presage and drive the development of midface hypoplasia in transition zone cilia mutants. While normal expression of *Shh* and *T* in the prechordal plate indicates that induction and specification of this tissue is not disrupted in transition zone mutants, reduced expression of *Gli1, Gsc,* and *FoxA2* suggests a disruption in autocrine signaling in this tissue compartment. Since no gross defects in ciliogenesis was observed in the prechordal plate, is this signaling defect a result of reduced ciliary localization of Hh pathway effectors such as Smoothened as observed in previous studies (Ben Chih et al., 2011; Dowdle et al., 2011; Garcia-Gonzalo et al., 2011)? Future studies are necessary to address this possibility.

Inductive paracrine signaling between adjacent tissue compartments is a common theme seen in the early development of many organs and structures in the embryo. Here, we add to the body of evidence showing a critical role in signaling from the prechordal plate to the adjacent neurectoderm in orchestrating development of the midface (Aoto et al., 2009; Dale et al., 1997; Kiecker & Niehrs, 2001; Marcucio et al., 2005; Rubenstein & Beachy, 1998). Our finding that early prechordal plate signaling defects in *Tctn2* mutants is followed by reduced *Shh* expression and reduced expression of Hh pathway transcriptional targets *Gli1* and *Ptch1* in the basal forebrain provides a spaciotemporal sequence for midfacial narrowing in these mutants. The exact mechanism for this defect in signal crosstalk still needs to be further clarified. One hypothesis is that canonical Hh pathway activation in the neurectoderm results in the expression of a transcription factor (or factors) that is required for the expression of *Shh* in the basal forebrain. One such candidate is the transcription factor Six3 which has been shown to be regulated by the Hh pathway and required for the induction of *Shh* in the developing forebrain (Geng et al., 2008; Jeong et al., 2008). Despite the intriguing possibility that reduced *Six3* could play a role in loss of *Shh* in the forebrain of *Tctn2* mutants, expression of this transcription factor was normal when assessed by WM-ISH and RT-qPCR analysis.

The data in this study indicates that increased cell death specifically in the neurectoderm and facial ectoderm is directly responsible for the midface hypoplasia seen in *Tctn2* mutants. This is consistent with published reports showing that loss/inhibition of Hh pathway components or pathway activation in the prechordal plate and/or neurectoderm results in increased cell death in the developing forebrain and facial ectoderm (Aoto et al., 2009; Aoto & Trainor, 2015; Marcucio et al., 2005). Interestingly, this cell death may be triggered via a Ptch1-induced pro-apoptotic

program activated in response to loss of the critical *Shh* domain in the basal forebrain that has been described in numerous studies (Aoto & Trainor, 2015; Fombonne et al., 2012; Mille et al., 2009; Thibert et al., 2003). Increased cleaved-caspase 9 and cleaved-caspase 3 staining in the basal forebrain and facial ectoderm of E9.5 *Tctn2* mutants provides support for this mechanism contributing to the midface defect. As numerous components of this Ptch1-induced apoptotic program have been identified, these provide attractive targets for potential phenotypic rescue in future studies.

The most surprising result of this study is the finding that reducing *Ptch1* gene dosage can fully rescue the midface defect in multiple transition zone cilia mutants (*Tctn2* and *Cc2d2a*). In light of the data showing that this phenotypic rescue is not due to restoration of *Shh* expression or Hh pathway activation in the basal forebrain a closer analysis of earlier data is necessary to explain how reducing *Ptch1* levels could alleviate the midface hypoplasia. It is possible that by reducing *Ptch1* levels this effectively brings it below a threshold concentration required for the induction of the pro-apoptotic program in absence of *Shh* in the basal forebrain. Future experiments to tease out this possibility will be extremely helpful in broadening our understanding of the non-canonical roles for Ptch1. It should also be noted that phenotypic rescue was limited to the midface defect in these transition zone mutants and did not extend to additional ciliopathy phenotypes in these embryos including polydactyly and microphthalmia. Insight into how the midface is preferentially more sensitive to small perturbations in *Ptch1* levels in comparison to other regions of the embryo will be of great interest for future studies.

The results of this study can be combined to form a simple model **(Figure 18)** to explain how transition zone disruption results in midface hypoplasia. **(1)** In normal development of the midface early signals from the prechordal plate are transmitted to the adjacent neurectoderm to regulate *Shh* and Hh pathway activation in that tissue to allow for cell survival and normal midface development. **(2)** When transition zone function of the primary cilium is disrupted, this impairs signal crosstalk between the prechordal plate and neurectoderm resulting in reduced *Shh* and Hh pathway activation in the basal forebrain to induce Ptch1-mediated apoptosis and culminating in midface collapse. **(3)** Decreasing *Ptch1* gene dosage rescues the midfacial narrowing by decreasing Ptch1-induced apoptosis despite a persisting decrease in *Shh* expression and Hh pathway activation in the neurectoderm of rescued embryos.

2.5 Materials and Methods

Mouse Strains

All mouse protocols were approved by the Institutional Animal Care and Use Committee (IACUC) at the University of California, San Francisco. *Tctn2*$^{+/-}$ (*Tctn2*$^{tm1.1Reit}$), *Cc2d2a*$^{+/-}$ (*Cc2d2a*$^{Gt(AA0274)Wtsi}$), *Tmem231*$^{+/-}$ (*Tmem231*$^{Gt(OST335874)Lex}$), and *Tmem67*$^{+/-}$ (*Tmem67*^{tm1Dgen}) mouse alleles have been previously described. *Wnt1-cre* (*Tg(Wnt1-cre)11Rth)* and *Islet1-cre* (*Isl1*$^{tm1(cre)Sev}$) mice were obtained from Brian Black, *Sox1-cre* (*Sox1*$^{tm1(cre)Take}$) mice were obtained from Jeff Bush, *Foxg1-cre* (*Foxg1*$^{tm1(cre)Skm}$) mice were obtained from Stavros Lomvardas, and *Crect-cre* (*Tg(Tcfap2a-cre)1Will)* mice were obtained from Trevor Williams. The *Ptch1*^{tm1Mps} allele was used in this study as a null allele. All mice were maintained on a C57BL/6J background. For timed matings, noon on the day a copulation plug was detected was considered to be 0.5 days postcoitus.

Immunofluorescence

The antibodies used in this study were rabbit α-Arl13b (1:1000, Proteintech 17711-1-AP), rabbit α-cleaved-caspase 3 (Asp175) (1:400, Cell Signaling #9664), rabbit α-cleaved-caspase 9 (Asp353) (1:100, Cell Signaling #9509), rabbit α-Phospho-Histone H3 (Ser28) (1:400, Cell Signaling #9713), chicken anti-GFP (1:1000, Aves labs GFP-1020), goat gamma-tubulin (1:200, Santa Cruz sc7396), rat E-Cadherin (1:1000, Invitrogen 13-1900), and rabbit FoxA2 (1:400 abcam ab108422). The In Situ Cell Death Detection Kit, Fluorescein (Roche) was used for TUNEL cell death assay. For immunofluorescence antibody staining of frozen tissue sections, embryos were fixed overnight in 4% PFA/PBS, washed in PBS and cryopreserved via overnight incubation in 30% sucrose/PBS. Embryos were embedded in OCT and frozen at -80C. Frozen OCT blocks were cut into 10μM sections. For immunostaining, frozen sections were washed

3x5’ in PBST (0.1%Tween-20/PBS) followed by blocking for 2 hours in blocking solution (5% donkey serum in PBS+ 0.3% Triton X-100 + 0.2% Na-azide). Slides were incubated overnight in primary antibody diluted in blocking solution at 4 degrees. The following day, slides were washed 3x10’ in PBST, stained with appropriate AlexaFluor 488, 568, or 647 conjugated secondary antibodies (Life Technologies) at 1:1000 and Hoecsht or Dapi nuclear stain in blocking buffer for 1 hour, rinsed 3x10’ with PBST and mounted using Fluoromount-G (Southern Biotech). All steps performed at room temperature unless otherwise noted. *Note: For gamma-tubulin antibody staining, antigen retrieval by incubating with 1%SDS/PBST for 5 mins prior to blocking and primary antibody incubation in required for good staining. Stained samples were imaged on a Leica SP-5 confocal microscope. Images were processed using FIJI (ImageJ).

In Situ Hybridization

Whole mount in situ hybridization was performed as previously described (Harrelson et al., 2012). DIG-labeled riboprobes were made using plasmids from the following sources: *Shh* (Echelard et al., 1993) , *Gsc* (Blum et al., 1992), *Ptch1* (Goodrich, 1999), *Foxa2* (Brennan et al., 2001), *Gli1* (EST W65013).

RT-qPCR

For gene expression studies, RNA was extracted from E8.5/E9.5 embryo heads using an RNAeasy Micro Kit (QIAGEN), and cDNA synthesis was performed using the iScript cDNA synthesis kit (BioRad). RT-qPCR was performed using EXPRESS Sybr GreenER 2X master mix with ROX (Invitrogen) and primers homologous to *Shh, Ptch1, Gli1,* or *Six3* on an ABI 7900HT real-time PCR machine. Expression levels were normalized to the geometric mean of three control genes (*Actb, Hprt,* and *Ubc)*, average normalized Ct values for control and experimental

groups determined and relative expression levels determined by ΔΔCt. The RT-qPCR of each RNA sample was performed in quadruplicate and each experiment was replicated.

Embryo processing for midface imaging

Embryos were harvested in ice-cold PBS, staged by counting somite number, and fixed o/n at 4 degrees in 4%PFA/PBS. Embryo heads were removed and stained in 0.01% ethidium bromide in PBS at room temperature for 15 minutes. Embryos were positioned using glass beads in PBS and imaged on a Leica MZ16 F fluorescence stereomicroscope.

Image Quantification

For 2D midface width quantification the infranasal distance was measure using FIJI software by drawing a line between the center of each nasal pit. For quantification of cell death and proliferation, 6 sections per embryo were quantified. Staining with epithelial marker E-cadherin was used for quantification of facial ectoderm while nuclear morphology was used to separate mesenchyme, hindbrain and forebrain tissue compartments. For quantification, threshold was first set for each image followed by binary watershed separation to obtain accurate nuclei counts. The percentage of TUNEL+ or pHH3+ nuclei were compared between *Tctn2* mutant and control samples.

Table 1. Primer sets used for RT-qPCR

Gene	Forward Primer	Reverse Primer
Actb	TTCTTTGCAGCTCCTTCGTT	ATGGAGGGGAATACAGCCC
Gli1	GGTGCTGCCTATAGCCAGTGTCCTC	GTGCCAATCCGGTGGAGTCAGACCC
Hprt	TCCTCCTCAGACCGCTTTT	CATAACCTGGTTCATCATCGC
Ptch1	CTCCTCATATTTGGGGCCTT	AATTCTCGACTCACTCGTCCA
Shh	CCAATTACAACCCCGACATC	GGCCAAGGCATTTAACTTGT
Six3	ACCACATCCTGGAGAACCAC	CTTCTCGGCCTCCTGGTAG
Ubc	TCCAGAAAGAGTCCACCCTG	GACGTCCAAGGTGATGGTCT
Xiap	GGTCCTGATTGCAGATCTTGT	CGCCTTAGCTGCTCTTCAGT

Table 2. Primer sets used for Genotyping Assays

Gene	Forward Primer	Reverse Primer
Cc2d2a	TGTCCTGGAGCTCCCTTCTA	TGCAGGCAATTTCTCTGTTG (wt) CTTCACATCCATGCTGAGGA (mut)
Cre (generic)	ACATTTGGGCCAGCTAAACAT	CGGCATCAACGTTTTCTTTT
Islet1:cre	CATTTCACTGTGGACATTACTCCC	ATCTTCAGGTTCTGCGGGAA
mTmG	CTCTGCTGCCTCCTGGCTTCT	CGAGGCGGATCACAAGCAATA (wt) TCAATGGGCGGGGGTCGTT (gt)
Ptch1	GCCTGAAGAACGAGATCAGC (mut) AGGGCTTCTCGTTGGCTACAA (wt)	GTTTCCCAGCTTCCCTTTTC (mut) CTGCGGCAAGTTTTTGGTTG (wt)
R26-EYFP	AAAGTCGCTCTGAGTTGTTAT	TAAGCCTGCCCAGAAGACTC (wt) GAAAGACCGCGAAGAGTTTG (mut)
Sox1:cre	GGCCCTCTCTTTGCGGTA	GGCAAACGGACAGAAGCATT
Tctn2	AGTGTGTCCTACTTAGGGCTTTTG (wt) CAGCAAGAACCATGTCTGGA (mut/cond)	TCCTTCAGTGGTGAACCTCAAC (wt) CTTCAGTGGTGAACCTCAACG (mut) ACGGGTGTCCTACATCCAAG (cond)
Tmem231	TCTAGGGAAACCTGGAGAAAC	GCATGCAAGGACTTAACCACT (wt) AGCTAGCTTGCCAAACCTACA (mut)
Tmem67	GGGTGGGATTAGATAAATGCCTGCTCT	GGCTATGGGTAGAATATTGTTCCAG (wt) GGACCTGGCGATTTGACGTCCTCAG (mut)

wt = wild-type allele
mut = mutant/null allele
cond = conditional allele

Chapter 3:

Where do we go from here?

3.1 Conclusion and Future Directions

The results of this study provide new insights into how the transition zone complex mediates cell-to-cell communication to mediate normal development of the midface. This work also contributes to the growing body of evidence suggesting various tissue-specific roles for primary cilia signaling leading to distinct outcomes in the various tissues comprising the craniofacial complex. In contrast to recent work showing a role for cilia in constraining proliferation of neural crest via Gli3 repressor in prevention of midface expansion and similar work indicating a role in specification of neural crest in prevention of maxillary hyperplasia and resulting high-arched palate, our work highlights a new role for cilia in craniofacial development originating in the prechordal plate (Brugmann et al., 2010a; Tabler et al., 2013). We have uncovered a new signaling paradigm whereby early signaling events from the prechordal plate are transduced to the adjacent neurectoderm in order to permit cell survival and expansion of neurectoderm and facial ectoderm cell types during midface development. While this work provides some detail of the molecular framework that coordinates this developmental process, as is common with scientific discovery many questions still arise.

One central finding of this study is the identification of the earliest molecular defect in the cascade of signaling events that ultimately give rise to midface hypoplasia: signaling defects in the prechordal plate. An unanswered question remains as to how cilia mediate autocrine signaling in the prechordal plate to regulate the expression of transcription factors *FoxA2* and *Gsc* as well as Hh pathway target *Gli1* in this tissue. One possibility is that the ciliary localization of key canonical Hh pathway components (e.g. Smoothened) is disrupted leading to defects in Gli transcription factor processing and reduced expression of these genes. One simple

way to test this hypothesis would be whole-embryo immunofluorescence staining for Smoothened receptor with co-staining for the ciliary marker acetylated-tubulin and quantification of Smoothened ciliary localization in the prechordal plate of *Tctn2* mutant and control embryos at E8.0. As preliminary attempts to stain for Smoothened in mouse tissue samples have been unsuccessful an alternative approach where Smoothened could be genetically labeled might be a better strategy to answer this question.

Another key result of this study is that reduced *Shh* expression in basal forebrain – a key signaling center for growth of the midface- is a main contributor to the midface defect observed in multiple transition zone mutants. How the transition zone complex mediates activation of *Shh* expression in this tissue remains enigmatic. I utilized a candidate approach to answer this question in this study by focusing on the transcription factor Six3 due to its documented role in regulating *Shh* in this tissue and because its expression is regulated via the Hh pathway. Although no defects were found in *Six3* expression in *Tctn2* mutants an unbiased approach would most likely provide a better strategy to answer this question. This could include RNA-seq or microarray studies in *Tctn2* mutant and control embryos at E9.0-E9.5, which corresponds to the developmental timepoint where *Shh* is reduced in the basal forebrain in mutant embryos. To gain the most useful data from these studies attention should be paid to ways in which samples could be purified to isolate specific tissues of interest (e.g. separation of neurectoderm, facial ectoderm, and neural crest). This strategy could be powerful in identifying key tissue-specific factors regulated by primary cilia signaling to coordinate midfacial development.

Our results add to the growing body of evidence supporting a non-canonical role for Ptch1

receptor in the direct activation of a pro-apoptotic program in the absence of ligand stimulation. This result identifies Ptch1 as an intriguing new target in developing new strategies aimed at combating midface defects caused by loss-of-function mutations in the Hh pathway and reduced ciliary signaling. A key feature of the Ptch1-induced apoptotic mechanism is cleavage of an intracellular C-terminal domain of the receptor that leads to direct cleavage and activation of Caspase-9 in the mitochondria. Could we rescue the midface defect in *Tctn2* mutants by mutating the Ptch1 intracellular residue required for cleavage and Caspase activation? If so, this would be powerful evidence confirming the involvement of this mechanism in the midface defects of transition zone mutants.

A key goal of this study was to identify in which tissue(s) of the craniofacial complex transition zone function is required to regulate midfacial development. Using a host of cre-drivers to delete *Tctn2* function in the neural crest, facial ectoderm, neurectoderm, and the prechordal plate we were unable to uncover tissue-specific deletion that recapitulates the midface narrowing seen in *Tctn2* null mutants. The results of this study suggest a role for Tctn2 in the prechordal plate and/or neurectoderm would be most critical for coordinating midface development. The persistence of Tctn2 function in the prechordal plate at E8.5 using the *Islet1-cre* drive and in the neurectoderm at E9.5 using the *Sox1-cre* driver evidenced by Arl13b ciliary localization indicates that the currently available tools for tissue-specific deletion are not active early enough to delete Tctn2 function at the critical timepoints necessary to dissect its role in early facial development. Development of new genetic tools could greatly assist in this endeavor. The transcription factor Gsc is known to be an early marker in the precordal plate and would be an attractive target to generate a prechordal plate-specific cre driver that would be active earlier than

the *Islet1-cre* driver while providing increased specificity for the prechordal plate. It would be very interesting to see if *Tctn2* deletion using a *Gsc-cre* driver could at least partially recapitulate the midface defect seen in *Tctn2* mutants.

The surprising result found in this study that reducing *Ptch1* gene dosage fully rescues the midface defects in transition zone mutants highlights new strategies to fix midface defects associated with defects in primary cilia signaling. One could imagine that another approach to rescue the midface defect would be replacing the lost *Shh* domain in the basal forebrain during early development. One way to do this would by employing an ex vivo whole embryo culture strategy of *Tctn2* mutant and control embryos in the presence of exogenously added Shh ligand. This exogenous addition of the missing ligand could effectively block Ptch1-induced apoptosis and restore normal midface development. Repeating this experiment with Smoothened agonist instead of Shh, which acts downstream of Ptch1, would be useful in teasing out whether this cell death mechanism occurs entirely through pathway separate and distinct from the canonical Shh-Smo-Gli pathway.

References

Ahdab-Barmada, M., & Claassen, D. (1990). A distinctive triad of malformations of the central nervous system in the Meckel-Gruber syndrome. *Journal of Neuropathology and Experimental Neurology*, *49*(6), 610–620.

Ahlgren, S. C., & Bronner-Fraser, M. (1999). Inhibition of sonic hedgehog signaling in vivo results in craniofacial neural crest cell death. *Current Biology : CB*, *9*(22), 1304–1314.

Anderson, C., & Stern, C. D. (2016). Organizers in Development. *Current Topics in Developmental Biology*, *117*, 435–454. http://doi.org/10.1016/bs.ctdb.2015.11.023

Aoto, K., & Trainor, P. A. (2015). Co-ordinated brain and craniofacial development depend upon Patched1/XIAP regulation of cell survival. *Human Molecular Genetics*, *24*(3), 698–713. http://doi.org/10.1093/hmg/ddu489

Aoto, K., Shikata, Y., Imai, H., Matsumaru, D., Tokunaga, T., Shioda, S., et al. (2009). Mouse Shh is required for prechordal plate maintenance during brain and craniofacial morphogenesis. *Developmental Biology*, *327*(1), 106–120. http://doi.org/10.1016/j.ydbio.2008.11.022

Baala, L., Audollent, S., Martinovic, J., Ozilou, C., Babron, M.-C., Sivanandamoorthy, S., et al. (2007). Pleiotropic effects of CEP290 (NPHP6) mutations extend to Meckel syndrome. *The American Journal of Human Genetics*, *81*(1), 170–179. http://doi.org/10.1086/519494

Baker, K., & Beales, P. L. (2009). Making sense of cilia in disease: The human ciliopathies. *American Journal of Medical Genetics Part A*, *151C*(4), 281–295. http://doi.org/10.1002/ajmg.c.30231

Ben Chih, Liu, P., Chinn, Y., Chalouni, C., Komuves, L. G., Hass, P. E., et al. (2011). A ciliopathy complex at the transition zone protects the cilia as a privileged membrane domain.

Nature, *14*(1), 61–72. http://doi.org/10.1038/ncb2410

Blum, M., Gaunt, S. J., Cho, K. W., Steinbeisser, H., Blumberg, B., Bittner, D., & De Robertis, E. M. (1992). Gastrulation in the mouse: the role of the homeobox gene goosecoid. *Cell*, *69*(7), 1097–1106.

Boycott, K. M., Parboosingh, J. S., Scott, J. N., McLeod, D. R., Greenberg, C. R., Fujiwara, T. M., et al. (2007). Meckel syndrome in the Hutterite population is actually a Joubert-related cerebello-oculo-renal syndrome. *American Journal of Medical Genetics Part A*, *143A*(15), 1715–1725. http://doi.org/10.1002/ajmg.a.31832

Brennan, J., Lu, C. C., Norris, D. P., Rodriguez, T. A., Beddington, R. S., & Robertson, E. J. (2001). Nodal signalling in the epiblast patterns the early mouse embryo. *Nature*, *411*(6840), 965–969. http://doi.org/10.1038/35082103

Brugmann, S. A., Allen, N. C., James, A. W., Mekonnen, Z., Madan, E., & Helms, J. A. (2010a). A primary cilia-dependent etiology for midline facial disorders. *Human Molecular Genetics*, *19*(8), 1577–1592. http://doi.org/10.1093/hmg/ddq030

Brugmann, S. A., Cordero, D. R., & Helms, J. A. (2010b). Craniofacial ciliopathies: A new classification for craniofacial disorders. *American Journal of Medical Genetics Part A*, *152A*(12), 2995–3006. http://doi.org/10.1002/ajmg.a.33727

Burdi, A. R. (2006). Developmental biology and morphogenesis of the face, lip and palate, 3–12.

Bush, J. O., & Jiang, R. (2012). Palatogenesis: morphogenetic and molecular mechanisms of secondary palate development. *Development (Cambridge, England)*, *139*(4), 828–828. http://doi.org/10.1242/dev.079152

Cahuana, A., Palma, C., Gonzáles, W., & Geán, E. (2004). Oral manifestations in Ellis-van Creveld syndrome: report of five cases. *Pediatric Dentistry*, *26*(3), 277–282.

Cakir, M., Mungan, I., Makuloglu, M., & Okten, A. (2006). Hydrocephalus with cleft lip and palate: an overlap between midline malformation syndromes. *Indian Journal of Pediatrics*, *73*(8), 731–733.

Cantagrel, V., Silhavy, J. L., Bielas, S. L., Swistun, D., Marsh, S. E., Bertrand, J. Y., et al. (2008). Mutations in the cilia gene ARL13B lead to the classical form of Joubert syndrome. *American Journal of Human Genetics*, *83*(2), 170–179. http://doi.org/10.1016/j.ajhg.2008.06.023

Chai, Y., & Maxson, R. E. (2006). Recent advances in craniofacial morphogenesis. *Developmental Dynamics*, *235*(9), 2353–2375. http://doi.org/10.1002/dvdy.20833

Chang, C. F., Schock, E. N., O'Hare, E. A., Dodgson, J., Cheng, H. H., Muir, W. M., et al. (2014). The cellular and molecular etiology of the craniofacial defects in the avian ciliopathic mutant talpid2. *Development (Cambridge, England)*, *141*(15), 3003–3012. http://doi.org/10.1242/dev.105924

Chiang, C., Litingtung, Y., Lee, E., Young, K. E., Corden, J. L., Westphal, H., & Beachy, P. A. (1996). Cyclopia and defective axial patterning in mice lacking Sonic hedgehog gene function. *Nature*, *383*(6599), 407–413. http://doi.org/10.1038/383407a0

Cohen, M. M., & Shiota, K. (2002). Teratogenesis of holoprosencephaly. *American Journal of Medical Genetics Part A*, *109*(1), 1–15. http://doi.org/10.1002/ajmg.10258

Corbit, K. C., Aanstad, P., Singla, V., Norman, A. R., Stainier, D. Y. R., & Reiter, J. F. (2005). Vertebrate Smoothened functions at the primary cilium. *Nature*, *437*(7061), 1018–1021. http://doi.org/10.1038/nature04117

Couly, G. F., Coltey, P. M., & Le Douarin, N. M. (1992). The developmental fate of the cephalic mesoderm in quail-chick chimeras. *Development (Cambridge, England)*, *114*(1), 1–15.

Cui, C., Chatterjee, B., Francis, D., Yu, Q., SanAgustin, J. T., Francis, R., et al. (2010). Disruption of Mks1 localization to the mother centriole causes cilia defects and developmental malformations in Meckel-Gruber syndrome. *Disease Models & Mechanisms*, *4*(1), 43–56. http://doi.org/10.1242/dmm.006262

Dale, J. K., Vesque, C., Lints, T. J., Sampath, T. K., Furley, A., Dodd, J., & Placzek, M. (1997). Cooperation of BMP7 and SHH in the induction of forebrain ventral midline cells by prechordal mesoderm. *Cell*, *90*(2), 257–269.

Danielian, P. S., Muccino, D., Rowitch, D. H., Michael, S. K., & McMahon, A. P. (1998). Modification of gene activity in mouse embryos in utero by a tamoxifen-inducible form of Cre recombinase. *Current Biology : CB*, *8*(24), 1323–1326.

Delous, M., Baala, L., Salomon, R., Laclef, C., Vierkotten, J., Tory, K., et al. (2007). The ciliary gene RPGRIP1L is mutated in cerebello-oculo-renal syndrome (Joubert syndrome type B) and Meckel syndrome. *Nature Genetics*, *39*(7), 875–881. http://doi.org/10.1038/ng2039

Dishinger, J. F., Kee, H. L., Jenkins, P. M., Fan, S., Hurd, T. W., Hammond, J. W., et al. (2010). Ciliary entry of the kinesin-2 motor KIF17 is regulated by importin-beta2 and RanGTP. *Nature Cell Biology*, *12*(7), 703–710. http://doi.org/10.1038/ncb2073

Dorn, K. V., Hughes, C. E., & Rohatgi, R. (2012). A Smoothened-Evc2 complex transduces the Hedgehog signal at primary cilia. *Developmental Cell*, *23*(4), 823–835. http://doi.org/10.1016/j.devcel.2012.07.004

Dowdle, W. E., Robinson, J. F., Kneist, A., Sirerol-Piquer, M. S., Frints, S. G. M., Corbit, K. C., et al. (2011). AR TICLEDisruption of a Ciliary B9 Protein Complex Causes Meckel Syndrome. *The American Journal of Human Genetics*, *89*(1), 94–110. http://doi.org/10.1016/j.ajhg.2011.06.003

Echelard, Y., Epstein, D. J., St-Jacques, B., Shen, L., Mohler, J., McMahon, J. A., & McMahon, A. P. (1993). Sonic hedgehog, a member of a family of putative signaling molecules, is implicated in the regulation of CNS polarity. *Cell*, *75*(7), 1417–1430.

Edvardson, S., Shaag, A., Zenvirt, S., Erlich, Y., Hannon, G. J., Shanske, A. L., et al. (2010). Joubert syndrome 2 (JBTS2) in Ashkenazi Jews is associated with a TMEM216 mutation. *American Journal of Human Genetics*, *86*(1), 93–97. http://doi.org/10.1016/j.ajhg.2009.12.007

Eggenschwiler, J. T., & Anderson, K. V. (2007). Cilia and Developmental Signaling. *Annual Review of Cell and Developmental Biology*, *23*(1), 345–373. http://doi.org/10.1146/annurev.cellbio.23.090506.123249

Endoh-Yamagami, S., Evangelista, M., Wilson, D., Wen, X., Theunissen, J.-W., Phamluong, K., et al. (2009). The mammalian Cos2 homolog Kif7 plays an essential role in modulating Hh signal transduction during development. *Current Biology : CB*, *19*(15), 1320–1326. http://doi.org/10.1016/j.cub.2009.06.046

Etchevers, H. C., Amiel, J., & Lyonnet, S. (2006). Molecular bases of human neurocristopathies. *Advances in Experimental Medicine and Biology*, *589*(Chapter 14), 213–234. http://doi.org/10.1007/978-0-387-46954-6_14

Fombonne, J., Bissey, P.-A., Guix, C., Sadoul, R., Thibert, C., & Mehlen, P. (2012). Patched dependence receptor triggers apoptosis through ubiquitination of caspase-9. *Proceedings of the National Academy of Sciences*, *109*(26), 10510–10515. http://doi.org/10.1073/pnas.1200094109

Foppiano, S., Hu, D., & Marcucio, R. S. (2007). Signaling by bone morphogenetic proteins directs formation of an ectodermal signaling center that regulates craniofacial development.

Developmental Biology, *312*(1), 103–114. http://doi.org/10.1016/j.ydbio.2007.09.016

Forni, P. E., Taylor-Burds, C., Melvin, V. S., Williams, T., & Wray, S. (2011). Neural Crest and Ectodermal Cells Intermix in the Nasal Placode to Give Rise to GnRH-1 Neurons, Sensory Neurons, and Olfactory Ensheathing Cells. *Journal of Neuroscience*, *31*(18), 6915–6927. http://doi.org/10.1523/JNEUROSCI.6087-10.2011

Fuccillo, M., Joyner, A. L., & Fishell, G. (2006). Morphogen to mitogen: the multiple roles of hedgehog signalling in vertebrate neural development. *Nature Reviews Neuroscience*, *7*(10), 772–783. http://doi.org/10.1038/nrn1990

Galdzicka, M., Patnala, S., Hirshman, M. G., Cai, J.-F., Nitowsky, H., Egeland, J. A., & Ginns, E. I. (2002). A new gene, EVC2, is mutated in Ellis-van Creveld syndrome. *Molecular Genetics and Metabolism*, *77*(4), 291–295.

Garcia-Gonzalo, F. R., & Reiter, J. F. (2012). Scoring a backstage pass: Mechanisms of ciliogenesis and ciliary access. *The Journal of Cell Biology*, *197*(6), 697–709. http://doi.org/10.1091/mbc.E08-07-0772

Garcia-Gonzalo, F. R., Corbit, K. C., Sirerol-Piquer, M. S., Ramaswami, G., Otto, E. A., Noriega, T. R., et al. (2011). A transition zone complex regulates mammalian ciliogenesis and ciliary membrane composition. *Nature Publishing Group*, *43*(8), 776–784. http://doi.org/10.1038/ng.891

Geng, X., Speirs, C., Lagutin, O., Inbal, A., Liu, W., Solnica-Krezel, L., et al. (2008). Haploinsufficiency of Six3 fails to activate Sonic hedgehog expression in the ventral forebrain and causes holoprosencephaly. *Developmental Cell*, *15*(2), 236–247. http://doi.org/10.1016/j.devcel.2008.07.003

Goetz, S. C., & Anderson, K. V. (2010). The primary cilium: a signalling centreduring vertebrate

development. *Nature Publishing Group*, *11*(5), 331–344. http://doi.org/10.1038/nrg2774

Goodrich, L. V. E. A. (1999). Overexpression of ptc1 Inhibits Induction of Shh Target Genes and Prevents Normal Patterning in the Neural Tube, 1–12.

Harrelson, Z., Kaestner, K. H., & Evans, S. M. (2012). Foxa2 mediates critical functions of prechordal plate in patterning and morphogenesis and is cell autonomously required for early ventral endoderm morphogenesis. *Biology Open*, *1*(3), 173–181. http://doi.org/10.1242/bio.2011040

Helms, D. H. A. J. A. (1999). SHH in facial morphogenesis, 1–12.

Helms, J. A. (2005). New insights into craniofacial morphogenesis. *Development (Cambridge, England)*, *132*(5), 851–861. http://doi.org/10.1242/dev.01705

Hébert, J. M., & McConnell, S. K. (2000). Targeting of cre to the Foxg1 (BF-1) Locus Mediates loxP Recombination in the Telencephalon and Other Developing Head Structures. *Developmental Biology*, *222*(2), 296–306. http://doi.org/10.1006/dbio.2000.9732

Hu, D. (2003). A zone of frontonasal ectoderm regulates patterning and growth in the face. *Development (Cambridge, England)*, *130*(9), 1749–1758. http://doi.org/10.1242/dev.00397

Hu, D., & Marcucio, R. S. (2008). A SHH-responsive signaling center in the forebrain regulates craniofacial morphogenesis via the facial ectoderm. *Development (Cambridge, England)*, *136*(1), 107–116. http://doi.org/10.1242/dev.026583

Hu, D., Young, N. M., Li, X., Xu, Y., Hallgrímsson, B., & Marcucio, R. S. (2015). A dynamic Shh expression pattern, regulated by SHH and BMP signaling, coordinates fusion of primordia in the amniote face. *Development (Cambridge, England)*, *142*(3), 567–574. http://doi.org/10.1242/dev.114835

Huangfu, D., & Anderson, K. V. (2005). Cilia and Hedgehog responsiveness in the mouse.

Proceedings of the National Academy of Sciences of the United States of America, *102*(32), 11325–11330. http://doi.org/10.1073/pnas.0505328102

Huangfu, D., Liu, A., Rakeman, A. S., Murcia, N. S., Niswander, L., & Anderson, K. V. (2003). Hedgehog signalling in the mouse requires intraflagellar transport proteins. *Nature*, *426*(6962), 83–87. http://doi.org/10.1038/nature02061

Hurd, T. W., Fan, S., & Margolis, B. L. (2011). Localization of retinitis pigmentosa 2 to cilia is regulated by Importin beta2. *Journal of Cell Science*, *124*(Pt 5), 718–726. http://doi.org/10.1242/jcs.070839

Jeong, Y., Leskow, F. C., El-Jaick, K., Roessler, E., Muenke, M., Yocum, A., et al. (2008). Regulation of a remote Shh forebrain enhancer by the Six3 homeoprotein. *Nature Genetics*, *40*(11), 1348–1353. http://doi.org/10.1038/ng.230

Jin, H., White, S. R., Shida, T., Schulz, S., Aguiar, M., Gygi, S. P., et al. (2010). The Conserved Bardet-Biedl Syndrome Proteins Assemble a Coat thatTraffics Membrane Proteins to Cilia. *Cell*, *141*(7), 1208–1219. http://doi.org/10.1016/j.cell.2010.05.015

Kee, H. L., Dishinger, J. F., Blasius, T. L., Liu, C.-J., Margolis, B., & Verhey, K. J. (2012). A size-exclusion permeability barrier and nucleoporins characterize a ciliary pore complex that regulates transport into cilia. *Nature Cell Biology*, *14*(4), 431–437. http://doi.org/10.1038/ncb2450

Kiecker, C., & Niehrs, C. (2001). The role of prechordal mesendoderm in neural patterning. *Current Opinion in Neurobiology*, *11*(1), 27–33.

Kim, J., Kato, M., & Beachy, P. A. (2009). Gli2 trafficking links Hedgehog-dependent activation of Smoothened in the primary cilium to transcriptional activation in the nucleus. *Proceedings of the National Academy of Sciences*, *106*(51), 21666–21671.

http://doi.org/10.1073/pnas.0912180106

Kim, S., & Dynlacht, B. D. (2013). Assembling a primary cilium. *Current Opinion in Cell Biology*, *25*(4), 506–511. http://doi.org/10.1016/j.ceb.2013.04.011

Knecht, A. K., & Bronner-Fraser, M. (2002). Induction of the neural crest: a multigene process. *Nature Reviews. Genetics*, *3*(6), 453–461. http://doi.org/10.1038/nrg819

Konstantinidou, A. E., Fryssira, H., Sifakis, S., Karadimas, C., Kaminopetros, P., Agrogiannis, G., et al. (2009). Cranioectodermal dysplasia: A probable ciliopathy. *American Journal of Medical Genetics Part A*, *149A*(10), 2206–2211. http://doi.org/10.1002/ajmg.a.33013

Kulaga, H. M., Leitch, C. C., Eichers, E. R., Badano, J. L., Lesemann, A., Hoskins, B. E., et al. (2004). Loss of BBS proteins causes anosmia in humans and defects in olfactory cilia structure and function in the mouse. *Nature Genetics*, *36*(9), 994–998. http://doi.org/10.1038/ng1418

Kyttälä, M., Tallila, J., Salonen, R., Kopra, O., Kohlschmidt, N., Paavola-Sakki, P., et al. (2006). MKS1, encoding a component of the flagellar apparatus basal body proteome, is mutated in Meckel syndrome. *Nature Genetics*, *38*(2), 155–157. http://doi.org/10.1038/ng1714

Litingtung, Y., & Chiang, C. (2000). Specification of ventral neuron types is mediated by an antagonistic interaction between Shh and Gli3. *Nature Neuroscience*, *3*(10), 979–985. http://doi.org/10.1038/79916

Liu, B., Chen, S., Johnson, C., & Helms, J. A. (2014). Reproductive Toxicology. *Reproductive Toxicology*, *48*, 88–97. http://doi.org/10.1016/j.reprotox.2014.05.009

Liu, B., Rooker, S. M., & Helms, J. A. (2010). Seminars in Cell & Developmental Biology. *Seminars in Cell and Developmental Biology*, *21*(3), 309–313. http://doi.org/10.1016/j.semcdb.2009.09.002

Loktev, A. V., & Jackson, P. K. (2013). Neuropeptide Y Family Receptors Traffic via the Bardet-Biedl Syndrome Pathway to Signal in Neuronal Primary Cilia. *CellReports*, *5*(5), 1316–1329. http://doi.org/10.1016/j.celrep.2013.11.011

Marcucio, R. S., Cordero, D. R., Hu, D., & Helms, J. A. (2005). Molecular interactions coordinating the development of the forebrain and face. *Developmental Biology*, *284*(1), 48–61. http://doi.org/10.1016/j.ydbio.2005.04.030

Maria, B. L., Boltshauser, E., Palmer, S. C., & Tran, T. X. (1999). Clinical features and revised diagnostic criteria in Joubert syndrome. *Journal of Child Neurology*, *14*(9), 583–90–discussion 590–1.

Mille, F., Thibert, C., Fombonne, J., Rama, N., Guix, C., Hayashi, H., et al. (2009). The Patched dependence receptor triggers apoptosis through a DRAL-caspase-9 complex. *Nature Cell Biology*, *11*(6), 739–746. http://doi.org/10.1038/ncb1880

Muenke, M., & Beachy, P. A. (2000). Genetics of ventral forebrain development and holoprosencephaly. *Current Opinion in Genetics & Development*, *10*(3), 262–269.

Nishimura, D. Y., Fath, M., Mullins, R. F., Searby, C., Andrews, M., Davis, R., et al. (2004). Bbs2-null mice have neurosensory deficits, a defect in social dominance, and retinopathy associated with mislocalization of rhodopsin. *Proceedings of the National Academy of Sciences of the United States of America*, *101*(47), 16588–16593. http://doi.org/10.1073/pnas.0405496101

Pedersen, L. B., & Rosenbaum, J. L. (2008). Intraflagellar Transport (IFT): Role in Ciliary Assembly, Resorption and Signalling. *Ciliary Function in Mammalian Development* (1st ed., Vol. 85, pp. 23–61). Elesvier Inc. http://doi.org/10.1016/S0070-2153(08)00802-8

Polymeropoulos, M. H., Ide, S. E., Wright, M., Goodship, J., Weissenbach, J., Pyeritz, R. E., et

al. (1996). The gene for the Ellis-van Creveld syndrome is located on chromosome 4p16. *Genomics*, *35*(1), 1–5. http://doi.org/10.1006/geno.1996.0315

Reid, B. S., Yang, H., Melvin, V. S., Taketo, M. M., & Williams, T. (2011). Ectodermal WNT/β-catenin signaling shapes the mouse face. *Developmental Biology*, *349*(2), 261–269. http://doi.org/10.1016/j.ydbio.2010.11.012

Roberson, E. C., Dowdle, W. E., Ozanturk, A., Garcia-Gonzalo, F. R., Li, C., Halbritter, J., et al. (2015). TMEM231, mutated in orofaciodigital and Meckel syndromes, organizes the ciliary transition zone. *The Journal of Cell Biology*, *209*(1), 129–142. http://doi.org/10.1083/jcb.201411087

Rohatgi, R., Milenkovic, L., & Scott, M. P. (2007). Patched1 Regulates Hedgehog Signaling at the Primary Cilium. *Science (New York, NY)*, *317*(5836), 372–376. http://doi.org/10.1126/science.1139740

Roume, J., Genin, E., Cormier-Daire, V., Ma, H. W., Mehaye, B., Attie, T., et al. (1998). A gene for Meckel syndrome maps to chromosome 11q13. *The American Journal of Human Genetics*, *63*(4), 1095–1101. http://doi.org/10.1086/302062

Rubenstein, J. L., & Beachy, P. A. (1998). Patterning of the embryonic forebrain. *Current Opinion in Neurobiology*, *8*(1), 18–26.

Ruiz-Perez, V. L., Blair, H. J., Rodriguez-Andres, M. E., Blanco, M. J., Wilson, A., Liu, Y. N., et al. (2007). Evc is a positive mediator of Ihh-regulated bone growth that localises at the base of chondrocyte cilia. *Development (Cambridge, England)*, *134*(16), 2903–2912. http://doi.org/10.1242/dev.007542

Ruiz-Perez, V. L., Ide, S. E., Strom, T. M., Lorenz, B., Wilson, D., Woods, K., et al. (2000). Mutations in a new gene in Ellis-van Creveld syndrome and Weyers acrodental dysostosis.

Nature Genetics, *24*(3), 283–286. http://doi.org/10.1038/73508

Santagati, F., & Rijli, F. M. (2003). Cranial neural crest and the building of the vertebrate head. *Nature Reviews Neuroscience*, *4*(10), 806–818. http://doi.org/10.1038/nrn1221

Sayer, J. A., Otto, E. A., O'toole, J. F., Nürnberg, G., Kennedy, M. A., Becker, C., et al. (2006). The centrosomal protein nephrocystin-6 is mutated in Joubert syndrome and activates transcription factor ATF4. *Nature Genetics*, *38*(6), 674–681. http://doi.org/10.1038/ng1786

Schock, E. N., Chang, C.-F., Struve, J. N., Chang, Y.-T., Chang, J., Delany, M. E., & Brugmann, S. A. (2015). Using the avian mutant talpid2 as a disease model for understanding the oral-facial phenotypes of oral-facial-digital syndrome. *Disease Models & Mechanisms*, *8*(8), 855–866. http://doi.org/10.1242/dmm.020222

Schwartz, R. S., Hildebrandt, F., Benzing, T., & Katsanis, N. (2011). Ciliopathies. *New England Journal of Medicine*, *364*(16), 1533–1543.

Shylo, N. A., Christopher, K. J., Iglesias, A., Daluiski, A., & Weatherbee, S. D. (2016). TMEM107 Is a Critical Regulator of Ciliary Protein Composition and Is Mutated in Orofaciodigital Syndrome. *Human Mutation*, *37*(2), 155–159. http://doi.org/10.1002/humu.22925

Smith, U. M., Consugar, M., Tee, L. J., McKee, B. M., Maina, E. N., Whelan, S., et al. (2006). The transmembrane protein meckelin (MKS3) is mutated in Meckel-Gruber syndrome and the wpk rat. *Nature Genetics*, *38*(2), 191–196. http://doi.org/10.1038/ng1713

Som, P. M., Streit, A., & Naidich, T. P. (2014). Illustrated review of the embryology and development of the facial region, part 3: an overview of the molecular interactions responsible for facial development. *AJNR. American Journal of Neuroradiology*, *35*(2), 223–229. http://doi.org/10.3174/ajnr.A3453

Spemann, H., & Mangold, H. (2001). Induction of embryonic primordia by implantation of organizers from a different species. 1923. *The International journal of developmental biology* (Vol. 45, pp. 13–38).

Sulik, K., Dehart, D. B., Iangaki, T., Carson, J. L., Vrablic, T., Gesteland, K., & Schoenwolf, G. C. (1994). Morphogenesis of the murine node and notochordal plate. *Developmental Dynamics*, *201*(3), 260–278. http://doi.org/10.1002/aja.1002010309

Susami, T., Kuroda, T., Yoshimasu, H., & Suzuki, R. (1999). Ellis-van Creveld syndrome: craniofacial morphology and multidisciplinary treatment. *The Cleft Palate-Craniofacial Journal : Official Publication of the American Cleft Palate-Craniofacial Association*, *36*(4), 345–352. http://doi.org/10.1597/1545-1569(1999)036<0345:EVCSCM>2.3.CO;2

Tabler, J. M., Barrell, W. B., Szabo-Rogers, H. L., Healy, C., Yeung, Y., Perdiguero, E. G., et al. (2013). Fuz Mutant Mice Reveal Shared Mechanisms between Ciliopathies and FGF-Related Syndromes. *Developmental Cell*, *25*(6), 623–635. http://doi.org/10.1016/j.devcel.2013.05.021

Thibert, C., Teillet, M.-A., Lapointe, F., Mazelin, L., Le Douarin, N. M., & Mehlen, P. (2003). Inhibition of neuroepithelial patched-induced apoptosis by sonic hedgehog. *Science (New York, NY)*, *301*(5634), 843–846. http://doi.org/10.1126/science.1085405

Tobin, J. L., & Beales, P. L. (2009). The nonmotile ciliopathies. *Genetics in Medicine*, *11*(6), 386–402. http://doi.org/10.1097/GIM.0b013e3181a02882

Tobin, J. L., Di Franco, M., Eichers, E., May-Simera, H., Garcia, M., Yan, J., et al. (2008). Inhibition of neural crest migration underlies craniofacial dysmorphology and Hirschsprung's disease in Bardet-Biedl syndrome. *Proceedings of the National Academy of Sciences*, *105*(18), 6714–6719. http://doi.org/10.1073/pnas.0707057105

Trainor, P. A., Tan, S. S., & Tam, P. P. (1994). Cranial paraxial mesoderm: regionalisation of cell fate and impact on craniofacial development in mouse embryos. *Development (Cambridge, England)*, *120*(9), 2397–2408.

Walczak-Sztulpa, J., Eggenschwiler, J., Osborn, D., Brown, D. A., Emma, F., Klingenberg, C., et al. (2010). REPOR TCranioectodermal Dysplasia, Sensenbrenner Syndrome, Is a Ciliopathy Caused by Mutations in the IFT122 Gene. *The American Journal of Human Genetics*, *86*(6), 949–956. http://doi.org/10.1016/j.ajhg.2010.04.012

Young, I. D. (1989). Cranioectodermal dysplasia (Sensenbrenner's syndrome). *Journal of Medical Genetics*, *26*(6), 393–396.

Young, N. M., Chong, H. J., Hu, D., Hallgrimsson, B., & Marcucio, R. S. (2010). Quantitative analyses link modulation of sonic hedgehog signaling to continuous variation in facial growth and shape. *Development (Cambridge, England)*, *137*(20), 3405–3409. http://doi.org/10.1242/dev.052340

Zaghloul, N. A., & Brugmann, S. A. (2011). The emerging face of primary cilia. *Genesis (New York, NY : 2000)*, *49*(4), 231–246. http://doi.org/10.1002/dvg.20728

Publishing Agreement

It is the policy of the University to encourage the distribution of all theses, dissertations, and manuscripts. Copies of all UCSF theses, dissertations, and manuscripts will be routed to the library via the Graduate Division. The library will make all theses, dissertations, and manuscripts accessible to the public and will preserve these to the best of their abilities, in perpetuity.

Please sign the following statement:

I hereby grant permission to the Graduate Division of the University of California, San Francisco to release copies of my thesis, dissertation, or manuscript to the Campus Library to provide access and preservation, in whole or in part, in perpetuity.

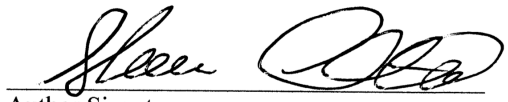

Author Signature

3/30/17

Date